Studies on function projective synchronization in chaotic and hyperchaotic systems

Thesis submitted to
Cochin University of Science and Technology
in partial fulfillment of the requirements
for the award of the degree of

Doctor of Philosophy

Sudheer Sebastian K
Department of Physics
Cochin University of Science and Technology
Kochi - 682022

June 2010

"Truth is ever to be found in the simplicity, and not in the multiplicity and confusion of things."

Isaac Newton

to my dearest Angelin and Benhur

CERTIFICATE

Certified that the work presented in this thesis is a bonafide work done by Mr. Sudheer Sebastian K, under my guidance in the Department of Physics, Cochin University of Science and Technology and that this work has not been included in any other thesis submitted previously for the award of any degree.

Kochi
June, 2010

Prof. M. Sabir
(Supervising Guide)

DECLARATION

I hereby declare that the work presented in this thesis is based on the original work done by me under the guidance of Prof. M. Sabir, Department of Physics, Cochin University of Science and Technology and has not been included in any other thesis submitted previously for the award of any degree.

Kochi
June, 2010

Mr.Sudheer Sebastian K

Acknowledgements

Let me praise God who gave me endurance and hope, the author and guide of my life. The dark moments came and went and I remained afloat.

I owe my deepest gratitude to my supervisor, Prof. M. Sabir, whose encouragement, guidance and support from the initial to the final level enabled me to develop an understanding of the subject and complete the research work in time.

I would like to express my gratitude to Prof. M. R. Anantharaman, Head of the Department of Physics for the valuable help and support. I thank him for providing necessary facilities for my research work.

I would also like to thank Dr. Ramesh Babu T for the valuable advice.

I thank all the faculty members of this department for the support they provided. The help and cooperation by the office staff and library staff is also gratefully acknowledged.

I thank the research scholars of the department Nima, Nijo, Tharanath, Priyesh, Vivek and Saneesh for their help and support. Special thanks are due to my colleague K. Y. Shaju for guidance and help.

I gratefully acknowledge the financial support provided by UGC, Govt. of India, in the form of teacher fellowship through FIP scheme.

I am extremely thankful to the Principal, the Manager and the Management of the Christ college, Irinjalakuda for permitting me to do Ph.D under the FIP scheme of UGC.

I am indebted to the head of the department and my colleagues in the Department of Physics Christ college, Irinjalakuda for their support. The help and cooperation by the office staff is also gratefully acknowledged.

I would like to acknowledge my gratitude to all my family members especially my parents and wife and children for their constant support and love.

Lastly, I offer my regards and blessings to all of those who supported me in any respect during the work of the thesis.

Sudheer Sebastian K

Contents

List of Figures

Preface

Chaotic systems are characterized by their extreme sensitivity to initial conditions, deterministic randomness and long term unpredictability. Since its introduction by Pecora and Carrol in 1990, chaos synchronization has received increasing attention due to its theoretical challenge and its great potential applications in secure communication, nano oscillators, chemical reactions, biological systems and so on. The idea of synchronization is to use the output of a master system to control a slave system so that the output of the response system follows the output of the master system asymptotically. Synchronization behaviour under bi-directional(mutual coupling) is also observed.

The concept of synchronization has been extended in scope to include a wide-ranging behaviour, such as complete synchronization, generalized synchronization, phase synchronization, lag synchronization, anti-phase synchronization, projective synchronization, modified projective synchronization etc.

Recently a few authors have studied a new type of synchronization called function projective synchronization(FPS). FPS is a more general definition of projective synchronization. As compared with projective synchronization, FPS means that the master and slave systems could be synchronized up to a scaling function $\alpha(t)$, but not a constant. This feature could be used to get more security in application to secure communications, because of the unpredictability of the scaling function in FPS.

More recently, a new type of synchronization phenomenon called modified function projective synchronization(MFPS) has been proposed. Here the responses of the synchronized dynamical states synchronize up to a desired scaling function matrix $\Lambda(t)$. The unpredictability involved in the scaling function matrix in MFPS can additionally enhance the security of communications.

Since the work of Pecora and Caroll synchronizing two identical chaotic systems with different initial conditions, a number of approaches have been proposed to achieve chaos synchronization. These include PC method, OGY method, scalar driving method, coupling control, manifold-based method, fuzzy control, impulsive-

control method , active control,adaptive control, time-delay feedback, open-plus-closed-loop(OPCL) control method etc. Of all these methods, active nonlinear control, adaptive nonlinear control and OPCL control methods have been extensively used recently for obtaining desired types of synchronization.

Recently, the study of synchronization in hyperchaotic systems has become a hot topic. A hyperchaotic system is defined as a chaotic system with at least two positive Lyapunov exponents, implying that its dynamics expand in several different directions simultaneously. This implies that hyperchaotic systems have more complex dynamical behaviors and could possibly be used in many fields such as chaos-based encryption, secure communication, biological systems, neural networks, etc.

This thesis is devoted to the study of FPS and MFPS of chaotic and hyperchaotic systems. A variety of methods like active nonlinear control, adaptive nonlinear control, and OPCL method are used to obtain function and modified function projective synchronization in chaotic systems like Lorenz system and Rössler systems. Hyperchaotic systems like Quantum-CNN oscillator, Chen system, Lü system, Lorenz system, and Rössler systems are also studied for FPS and MFPS.

Chapter 1 gives an introduction to chaos theory and synchronization in chaotic systems. Various synchronization phenomena and different methods of obtaining desired types of synchronization are discussed. Numerical method of solving nonlinear ODE's is also given.

Chapter 2 is devoted to the study of FPS in two identical hyperchaotic systems. Active nonlinear control method is employed to obtain the FPS of hyperchaotic Lü system. The active nonlinear control functions are properly designed so that the error system for FPS has all eigenvalues with negative real parts. Numerical simulations are used to verify the effectiveness of the proposed control techniques. We show that the active nonlinear control method produces robust FPS.

Chapter 3 deals with FPS of two-cell Quantum-CNN(Cellular Nonlinear Network) oscillators. Recently, Q-CNN oscillators have attracted attention of scientists and engineers as a nano scale chaos generator. Adaptive nonlinear controllers are designed based on Lyapunove stability theorem to obtain FPS of two-cell Quantum-CNN oscillators. The parameters of the slave system are assumed to be unknown. Adaptive nonlinear controllers and parameter update rules are derived to obtain FPS under parameter uncertainty. Numerical simulations are performed to verify the effectiveness of the proposed controllers.

MFPS between hyperchaotic Lorenz system and Lü system is considered in **chapter 4**. Parameters of both the systems are unknown. On the basis of Lyapunov stability theory, we design adaptive synchronization controllers with corresponding parameter update laws to synchronize the two systems. All the theoretical results are

verified by numerical simulations to demonstrate the effectiveness of the proposed synchronization schemes.

Chapter 5 studies FPS of some representative systems like Lorenz system, Rössler system, hyperchaotic Lorenz system and hyperchaotic Chen through OPCL coupling. This method gives precise driving for any continuous system in order to reach any desired dynamics. Numerical simulations show that OPCL coupling can provide stable FPS in identical and mismatched chaotic systems.

Chapter 6 presents MFPS of hyperchaotic systems through OPCL coupling. MFPS of identical hyperchaotic Rössler and mismatched hyperchaotic Lü systems are also studied through OPCL coupling. Possible application of MFPS in secure communication is also presented.

In **Chapter 7** the results are summarized.

Part of these investigations has been published in journals and presented in conferences.

List of publications

1. **K.S. Sudheer** and M. Sabir, Hybrid synchronization of hyperchaotic Lü system, Pramana,Journal of physics 73, 781(2009).

2. **K.S. Sudheer** and M. Sabir, Adaptive function projective synchronization of two-cell Quantum-CNN chaotic oscillators with uncertain parameters, Physics Letters A 373, 1847(2009).

3. **K.S. Sudheer** and M. Sabir, Adaptive modified function projective synchronization between hyperchaotic Lorenz system and hyperchaotic Lü system with uncertain parameters, Physics Letters A 373, 3743(2009).

4. **K.S. Sudheer** and M. Sabir, Switched modified function projective synchronization of hyperchaotic Qi system with uncertain parameters, Communications in Nonlinear Science and Numerical Simulations 15, 4058(2010).

5. **K.S. Sudheer** and M. Sabir, Function projective synchronization in chaotic and hyperchaotic systems through Open-Plus-Closed-Loop coupling, Chaos 20, 013115(2010).

6. **K.S. Sudheer** and M. Sabir, Modified function projective synchronization of hyperchaotic systems through Open-Plus- Closed-Loop coupling, Physics Letters A 374, 2017(2010).

School/Workshop/Conferences attended

1. DST-SERC School on Nonlinear Dynamics, June 26 - July 16, 2008, IISc Mathematics Initiative (IMI), Indian Institute of Science, Bangalore - 560012, INDIA

2. International Conference on Nonlinear Dynamical Systems and Turbulence July 17 - 22, 2008, Indian Institute of Science, Bangalore - 560012, INDIA

3. NCNSD -2009,March 5-7, 2009, Saha Institute of Nuclear Physics 1/AF, Bidhannagar Kolkata - 700 064.

4. International Workshop on Delayed Complex Systems (October 5 9, 2009) Max Planck Institute for physics of complex systems, Dresden, Germany.

Chapter 1

Introduction

> "It may happen that small differences in the initial conditions produce very great ones in the final phenomena. A small error in the former will produce an enormous error in the latter. Prediction becomes impossible." —— Henri Poincaré

Many dynamical systems in Physics, Chemistry and biology exhibit complex behaviour. Lasers, nano oscillators, vibrating structures, electronic oscillators, magnetic devices, chemical oscillators, and population kinetics can behave in a complicated manner. One can find irregular motion when long time prediction is not possible. For all these systems we have good mathematical models in forms of deterministic nonlinear differential or difference equations. "Deterministic" means that no stochastic forces enter the equations. The theoretical and experimental studies of these systems show that for many nonlinear or piece-wise linear systems the time history is sensitive to initial conditions and that a precise knowledge of the future behaviour is not possible. Nearby trajectories diverge from each other exponentially in time. This behaviour is called " chaos" in literature.

1.1 Chaotic dynamics

1.1.1 History

Chaotic dynamics may have had its beginnings in the work of the French mathematical physicist Henri Poincare in the late 1800's [1]. Poincare attempted to solve the celestial three-body problem(Sun, planet and moon) experiencing mutual gravitational pull. He was able to show that the three-body problem has complicated orbital dynamics which we now call chaos.

In 1927, Van der Pol [2]reported "irregular noise" in a radio circuit driven at

certain frequencies, but considered it a subsidiary phenomenon. Cartwright and Littlewood [3], alerted to a model of Van der Pol's circuit by the British Radio Research Board, identified "random-like" dynamics in the equations. These papers came to the attention of Smale[5], who developed the Smale horseshoe as a simplest reduction of Levinson's [4] observations. Smale's important insight unified the homoclinic behavior found by Poincare in celestial mechanics with Van der Pol's noisy oscillator.

At about the same time, in the early 1960's, the meteorologist Lorenz[6] was trying to understand the failures of linear prediction techniques for weather forecasts. Using one of the world's first mass-produced computers to simulate atmospheric dynamics, he found that long time aperiodic trajectories could be produced quite robustly. Then he found that the aperiodicity was paired with sensitive dependence on initial conditions.

With the help of Saltzman, he reduced the atmosphere simulation to a differential equation in three variables that produced the Lorenz attractor .Lorenz later gave a lecture entitled "Predictability: Does the Flap of a Butterfly's Wings in Brazil set off a Tornado in Texas?", which caused the concept of sensitive dependence on initial conditions to become popularly known as the "butterfly effect".

Also in the 1960's , Ueda [7]posed a mathematical model on an analog computer(i.e vacuum tubes) that displayed chaotic dynamics.

In 1975, Yorke and Li [8]showed that sustained aperiodic behavior could be found in one-dimensional maps. They coined the term chaos for the various phenomena that showed aperiodicity along with sensitive dependence on initial conditions. In addition to showing that the existence of a period-three orbit in a one-dimensional continuous map implies sensitive dependence, they showed another remarkable consequence: the existence of infinitely many other periodic orbits. In 1976 May[9] presented the logistic map as a plausible population model with a period-doubling cascade of bifurcations and chaotic trajectories.

Around the same time, Gollub and Swinney[10] reported aperiodic dynamics in a flow between rotating cylinders, in an attempt to explain the transition from laminar flow to turbulence. Toward the same goal, Libchaber demonstrated a period-doubling cascade in a convective Rayleigh-Benard experiment a few years later. Since then, experiments in a wide array of scientific and engineering disciplines have been designed that clearly display the effects of deterministic chaos.

The main catalyst for the development of chaos theory was the electronic computer. Much of the mathematics of chaos theory involves the repeated iteration of simple mathematical formulas, which would be impractical to do by hand. Electronic computers made these repeated calculations practical, while computer gener-

ated figures and images made it possible to visualize these systems.The availability of cheaper, more powerful computers broadens the applicability of chaos theory. Currently, chaos theory continues to be a very active area of research, involving many different disciplines such as mathematics, physics, chemical systems, population studies, biology, meteorology, astrophysics, information theory, etc.

1.1.2 A definition of chaos

Although there is no universally accepted definition of chaos, a commonly-used definition is[11]:

"Chaos is the phenomenon of occurrence of bounded nonperiodic evolution in completely deterministic nonlinear dynamical systems with high sensitive dependence on initial conditions"

Mathematically ,for a dynamical system to be classified as chaotic, it must have the following properties[12]:

1. it must be sensitive to initial conditions
2. it must be topologically mixing, and
3. its periodic orbits must be dense.

Sensitivity to initial conditions

Sensitivity to initial conditions means that each point in such a system is arbitrarily closely approximated by other points with significantly different future trajectories. Thus, an arbitrarily small perturbation of the current trajectory may lead to significantly different future behaviour. The Lyapunov exponent characterises the extent of the sensitivity to initial conditions. Quantitatively, two trajectories in phase space with initial separation δZ_0 diverge

$$|\delta Z(t)| \approx e^{\lambda t}|\delta Z_0| \tag{1.1}$$

if λ the Lyapunov exponent is positive. The rate of separation can be different for different orientations of the initial separation vector. Thus, a system has as many Lyapunov exponents as the number of dimensions of the phase space. A system which has one positive Lyapunov exponent is called a chaotic system. Hyperchaotic systems have more than one positive Lyapunov exponent.

Topological mixing

Topological mixing (or topological transitivity) means that the system will evolve over time so that any given region or open set of its phase space will eventually

overlap with any other given region.

Density of periodic orbits

Density of periodic orbits means that every point in the space is approached arbitrarily closely by periodic orbits. Topologically mixing systems not satisfying this condition may not display sensitivity to initial conditions, and hence may not be chaotic.

1.2 Chaos Synchronization

Christiaan Huygens was to first observe anti-phase synchronization of two pendulum clocks, with a common frame, in 1665. Huygens found that the pendulum clocks swung at exactly the same frequency and 180° out of phase. When he disturbed one pendulum the antiphase state was restored within half an hour and pendulum clocks remained synchronized indefinitely, thereafter, if left undisturbed. He found that synchronization did not occur when the clocks were separated beyond a certain distance, or oscillated in mutually perpendicular planes. Huygens deduced that the crucial interaction came from very small movements of the common frame supporting the two clocks. He also provided a physical explanation for how the frame motion set up the anti-phase motion [13].Synchronization in regular and periodic systems is a well developed topic.

Chaotic systems are dynamical systems that, apparently, defy synchronization due to their essential sensitivity to initial conditions. Consequently, two identical chaotic systems starting at closely initial conditions becomes uncorrelated in the course of time. Nevertheless it has been shown that it is possible to synchronize these kind of systems. The synchronization of chaotic systems is a subject with beginning in the early 80's but has become a hot topic in the last decade due to its potential use for secure communications[14], nano oscillators[15] and biological systems[16].

Fujisaka and Yamada [17]-[20] did early work on synchronization of chaotic systems, but it was not until the work of Pecora and Carroll [21, 22] that the subject received a significant amount of attention. The term 'chaotic synchronization' refers to a variety of phenomena in which chaotic systems adjust a given property of their motion to a common behaviour due to a coupling or to a driving force[23, 24]. The systems might be identical or different, the coupling might be unidirectional (master–slave or drive–response coupling) or bi-directional (mutual coupling) and the driving force might be deterministic or stochastic. Two systems are coupled

unidirectionally if the dynamics of one system (called master or drive) affects the dynamics of the other (called slave or response), while the dynamics of the slave does not affect the dynamics of the master. The fact that two unidirectionally coupled chaotic systems can be used in a secure communication scheme was first shown by Cuomo and Oppenheim [25, 26], who built a circuit version of the Lorenz equations and showed the possibility of using this system to transmit a small speech signal. While some years ago the word 'chaos' had a negative connotation in applied research, now a days researchers are developing techniques for taking advantage of chaotic dynamics instead of trying to avoid it. The use of chaos synchronization in secure communication systems is a good example of this more recent point of view.

1.3 Different types of synchronization

In the case of coupled dynamical systems, a number of different synchronization states have been studied. These include complete synchronization(CS)[21, 27], generalized synchronization(GS)[28, 29],phase synchronization (PS)[30, 31],antiphase synchronization (APS)[32, 33], lag synchronization (LS)[32, 33], projective synchronization(PS)[36]-[42],and modified projective synchronization(MPS)[49]-[53] etc. CS appears as the equality of the state variables while evolving in time. The GS introduced for drive- response systems, means that there is some functional relation between coupled chaotic oscillators, i.e., $x_2(t) = F[x_1(t)]$. In the case of LS where the states of the two oscillators are nearly identical, one system lags in time relative to the other, i.e., $x_2(t) = x_1(t + \tau)$. PS is an intermediate case characterized by the asymptotic boundness of the phase difference of the two outputs, the two chaotic amplitudes remaining uncorrelated. Recently, it has been shown that phase, generalized lag, and complete synchronization are closely connected with each other and, as a matter of fact, they are different manifestations of one type of synchronous oscillation behaviour of coupled chaotic oscillators called time-scale synchronization[54]-[58].

1.3.1 Projective synchronization

Among all kinds of chaos synchronization, projective synchronization, where the master and slave vectors synchronize up to a constant scaling factor α has been extensively investigated in recent years. The projective synchronization in unidirectionally coupled chaotic systems is described below.

Consider the following master and slave system

$$\dot{\mathbf{x}} = \mathbf{f}(\mathbf{x}) \tag{1.2}$$

$$\dot{\mathbf{y}} = \mathbf{g}(\mathbf{y}) + \mathbf{u}(\mathbf{x}, \mathbf{y}) \tag{1.3}$$

where $\mathbf{x}, \mathbf{y} \in \mathbf{R}^n$ are the state vectors, $\mathbf{f}, \mathbf{g} : \mathbf{R}^n \to \mathbf{R}^n$ are continuous nonlinear vector functions, $\mathbf{u}(\mathbf{x}, \mathbf{y})$ is the vector controller. We define the error system as

$$\mathbf{e}(\mathbf{t}) = \mathbf{y}(\mathbf{t}) - \alpha \mathbf{x}(\mathbf{t})$$

where α is a constant.

The systems (1.2) and (1.3) are said to be in projective synchronization, if there exists a constant α such that $\lim_{t\to\infty} \|\mathbf{e}(t)\| = 0$.

Complete synchronization can be regarded as a special case of projective synchronization characterized by $\alpha = 1$, and anti-phase synchronization characterized by $\alpha = -1$. This proportionality feature can be used to extend binary digital communication to M-nary digital communication for achieving fast communication[45]-[48]. Projective synchronization was first reported by Mainieri and Rehacek [36] in partially linear systems, where the responses of two identical systems synchronize up to a constant scaling factor. Xu [37] showed that the scaling factor of projective synchronization in coupled partially linear systems is unpredictable and can be arbitrarily maneuvered by introducing a feedback control to the master system. Xu and co-authors further introduced several control schemes [38, 39] based on Lyapunov stability theory to conduct the scaling factor onto a desired value, and derived a general condition [40, 41] for projective synchronization. Generalized projective synchronization was reported [42]-[44], in the study of a general class of chaotic systems without the limitation of partial-linearity.

1.3.2 Modified Projective synchronization

Modified projective synchronization[49]-[53] was proposed by Li in [49, 50], where the drive and response systems could be synchronized to a constant scaling matrix. Modified projective synchronization in chaotic systems is defined below.

Consider the following master and slave system

$$\dot{\mathbf{x}} = \mathbf{f}(\mathbf{x}) \tag{1.4}$$

$$\dot{\mathbf{y}} = \mathbf{g}(\mathbf{y}) + \mathbf{u}(\mathbf{x}, \mathbf{y}) \tag{1.5}$$

where $\mathbf{x}, \mathbf{y} \in \mathbf{R}^n$ are the state vectors, $\mathbf{f}, \mathbf{g} : \mathbf{R}^n \to \mathbf{R}^n$ are continuous nonlinear vector functions, $\mathbf{u}(\mathbf{x}, \mathbf{y})$ is the vector controller. We define the error system as

$$\mathbf{e}(t) = \mathbf{y}(\mathbf{t}) - \Lambda \mathbf{x}(\mathbf{t}) \tag{1.6}$$

where Λ is a $n \times n$ diagonal matrix, i.e $\Lambda(t) = diag(\alpha_1, \alpha_2, ..., \alpha_n)$, and α_i are constant scaling factors.

The system (1.4) and (1.5) are said to be in modified projective synchronization, if there exists a constant scaling matrix Λ such that $\lim_{t\to\infty} \|\mathbf{e}(t)\| = 0$.

By choosing the scaling factors in the scaling matrix, one can flex the scales of the different states independently.

Hybrid synchronization

Hybrid synchronization is an interesting case where one part of the system is anti-synchronized and the other completely synchronized so that complete synchronization (CS) and anti-synchronization(AS) co-exist in the system. This is a special case of modified projective synchronization and has been investigated in [59].

1.3.3 Function projective synchronization

Recently a few authors have proposed a new type of synchronization called function projective synchronization(FPS)[60]-[61]. FPS generalizes projective synchronization. In this scheme the master and slave systems are synchronized up to a scaling function $\alpha(t)$, which is not a constant.

Consider the following master and slave system

$$\dot{\mathbf{x}} = \mathbf{f}(\mathbf{x}) \tag{1.7}$$

$$\dot{\mathbf{y}} = \mathbf{g}(\mathbf{y}) + \mathbf{u}(\mathbf{x}, \mathbf{y}) \tag{1.8}$$

where $\mathbf{x}, \mathbf{y} \in \mathbf{R}^n$ are the state vectors, $\mathbf{f}, \mathbf{g} : \mathbf{R}^n \to \mathbf{R}^n$ are continuous nonlinear vector functions, $\mathbf{u}(\mathbf{x}, \mathbf{y})$ is the vector controller. We define the error system as

$$\mathbf{e}(\mathbf{t}) = \mathbf{y}(\mathbf{t}) - \alpha(t)\mathbf{x}(\mathbf{t})$$

where $\alpha(t)$ is a continuously differentiable function with $\alpha(t) \neq 0$ for all t.

The system (1.7) and (1.8) are said to be in FPS, if there exists a scaling function $\alpha(t)$ such that $\lim_{t\to\infty} \|\mathbf{e}(t)\| = 0$.

The freedom of choosing the scaling function in FPS is an advantage and can additionally enhance the security of communication.

1.3.4 Modified Function projective synchronization

More recently, a new type of synchronization scheme, modified function projective synchronization (MFPS)[62], has been developed. In this method the responses

of the synchronized dynamical states synchronize up to a desired scaling function matrix $\Lambda(t)$. MFPS is more general than modified projective synchronization and FPS.

Consider the following master and slave system

$$\dot{\mathbf{x}} = \mathbf{f}(\mathbf{x}) \tag{1.9}$$

$$\dot{\mathbf{y}} = \mathbf{g}(\mathbf{y}) + \mathbf{u}(\mathbf{x}, \mathbf{y}) \tag{1.10}$$

where $\mathbf{x}, \mathbf{y} \in \mathbf{R}^n$ are the state vectors, $\mathbf{f}, \mathbf{g} : \mathbf{R}^n \rightarrow \mathbf{R}^n$ are continuous nonlinear vector functions, $\mathbf{u}(\mathbf{x}, \mathbf{y})$ is the vector controller. We define the error system as

$$\mathbf{e}(t) = \mathbf{x}(\mathbf{t}) - \Lambda(t)\mathbf{y}(\mathbf{t}) \tag{1.11}$$

where $\Lambda(t)$ is a $n \times n$ order diagonal matrix, i.e $\Lambda(t) = diag(\alpha_1(t), \alpha_2(t), ..., \alpha_n(t))$, and $\alpha_i(t)$ is a continuous differentiable function with $\alpha_i(t) \neq 0$ for all t.

The systems (1.9) and (1.10) are said to be in MFPS, if there exists a scaling function matrix $\Lambda(t)$ such that $\lim_{t\rightarrow\infty} \|\mathbf{e}(t)\| = 0$.

It is obvious that compared with FPS, the MFPS can provide more security in communication.

1.4 Different methods for obtaining synchronization

Since Pecora and Caroll synchronized two identical chaotic systems with different initial conditions [21, 22], a number of approaches have been proposed to achieve chaos synchronization. These include Ott- Grebogi-Yorke(OGY) method[63, 64], scalar driving method[65, 66], coupling control[67, 68], manifold-based method[69, 70], fuzzy control[71, 72], impulsive-control method [73, 74], active control[75]-[85], adaptive control[86]-[100], time-delay feedback[102, 103] and Open-Plus-Closed-Loop control method(OPCL) [104, 105] etc.

Of all these methods, active nonlinear control, adaptive nonlinear control and OPCL control methods have been extensively used in recent literature for obtaining various types of synchronization.

1.4.1 Active nonlinear control method

The active control scheme proposed by Bai and Lonngren [75]-[76] has received considerable attention during the last decade. Applications to various systems abound, some of which include Rössler and Chen system[77], the electronic circuits which

model a third-order "jerk' equation [78], Lorenz, Chen and Lü system [79], geophysical model [80], nuclear magnetic resonance (NMR) modelled by the nonlinear Bloch equations [81],RCL-shunted Josephson junction [82], inertial ratchets [83],[84] and most recently in extended Bonhoffer-Van der Pol oscillator [85].

The method of synchronizing two identical chaotic systems through active nonlinear control method can be illustrated using chaotic Lorenz system. The Lorenz system is described by following set of nonlinear differential equations.

$$\begin{aligned} \dot{x} &= \sigma(y-x) \\ \dot{y} &= rx - y - xz \\ \dot{z} &= xy - bz \end{aligned} \tag{1.12}$$

The system is chaotic for the parameter values $\sigma = 10$, $r = 28$ and $b = 8/3$.

We assume that we have two Lorenz systems and that the system with the subscript 1 (master) is to control the system with the subscript 2 (slave). The systems are :

$$\begin{aligned} \dot{x}_1 &= \sigma(y_1 - x_1) \\ \dot{y}_1 &= rx_1 - y_1 - x_1 z_1 \\ \dot{z}_1 &= x_1 y_1 - b z_1 \end{aligned} \tag{1.13}$$

and

$$\begin{aligned} \dot{x}_2 &= \sigma(y_2 - x_2) + u_1 \\ \dot{y}_2 &= rx_2 - y_2 - x_2 z_2 + u_2 \\ \dot{z}_2 &= x_2 y_2 - b z_2 + u_3 \end{aligned} \tag{1.14}$$

Here u_1, u_2 and u_3 are control functions to be determined for obtaining desired type of synchronization. For complete synchronization, the error states are defined as

$$\begin{aligned} e_1 &= x_2 - x_1 \\ e_2 &= y_2 - y_1 \\ e_3 &= z_2 - z_1 \end{aligned} \tag{1.15}$$

The error dynamical system obtained from (1.13) and (1.14) is

$$\begin{aligned} \dot{e}_1 &= \sigma(e_2 - e_1) + u_1 \\ \dot{e}_2 &= re_1 - e_2 - x_2z_2 + x_1z_1 + u_2 \\ \dot{e}_3 &= x_2y_2 - x_1y_1 - be_3 + u_3 \end{aligned} \tag{1.16}$$

We define the active control functions u_1, u_2 and u_3 as

$$\begin{aligned} u_1 &= v_1 \\ u_2 &= x_2z_2 - x_1z_1 + v_2 \\ u_3 &= -x_2z_2 + x_1y_1 + v_3 \end{aligned} \tag{1.17}$$

where $v_i(t), i = 1, 2, 3$ are to be determined. Substitution of this leads to

$$\begin{aligned} \dot{e}_1 &= \sigma(e_2 - e_1) + v_1 \\ \dot{e}_2 &= re_1 - e_2 + v_2 \\ \dot{e}_3 &= -be_3 + v_3 \end{aligned} \tag{1.18}$$

Equation (1.18) describes the error dynamics and can be considered as a control problem where the system to be controlled is a linear system with a control input v_1, v_2 and v_3 as functions of e_1, e_2 and e_3. There are many possible choices for the control v_1, v_2 and v_3. We choose

$$\begin{bmatrix} v_1 \\ v_2 \\ v_3 \end{bmatrix} = A \begin{bmatrix} e_1 \\ e_2 \\ e_3 \end{bmatrix} \tag{1.19}$$

where A is a 3×3 constant matrix. For (1.18) to be asymptotically stable, the elements of the matrix A are properly chosen so that the closed loop system(1.18) will have all eigen values with negative real parts. Various choices of A are possible. A good choice is

$$A = \begin{bmatrix} \sigma - 1 & -\sigma & 0 \\ -r & 0 & 0 \\ 0 & 0 & b - 1 \end{bmatrix} \tag{1.20}$$

For this particular choice, the closed loop system (1.18)has eigenvalues that are found to be $-1, -1$ and -1. This choice will lead to a stable system and the synchronization of two Lorenz systems.

The active nonlinear control method realizes robust synchronization of two iden-

tical chaotic systems. The method is simple and easy to implement in practical applications. In chapter 2, we present our studies on hybrid synchronization and FPS in hyperchaotic Lü system using active control method.

1.4.2 Adaptive nonlinear control method

In active control method, it is essential to know the parameters of the model for the derivation of the controller. In practical situations, these parameters may be unknown. Moreover, these parameters may change from time to time. Thus the derivation of adaptive controller for the synchronization of chaotic systems in the presence of system parameter uncertainty is an important problem[86]-[96]. Synchronization of two different chaotic systems is also a challenging problem [97]-[100].

A general method of designing adaptive nonlinear controller and parameter update rule for synchronization of two chaotic(hyperchaotic) systems is described below.

Consider an n_1-dimensional chaotic(hyperchaotic) system in the form of

$$\dot{x} = F(x, p), \tag{1.21}$$

where $x = (x_1, x_2, ..., x_{n_1})^T \in R^{n_1}$, and the unknown parameters $p \in R^{m_1}$. Assume that the structure of the chaotic(hyperchaotic) dynamical system, $F(x, p) = (F_1(x, p), F_2(x, p), ..., F_{n_1}(x, p))^T$, is known, and time series for all variables are available as output of (1.21). We refer to (1.21) as the drive system, and the response system is given by

$$\dot{y} = G(y, q) + u(x, y, \hat{p}, \hat{q})), \tag{1.22}$$

where $y = (y_1, y_2, ...y_{n_2})^T \in R^{n_2}(n_2 \leq n_1)$, the unknown parameters $q \in R^{n_2}$, and the dynamical evolution equations, $G(y, q) = (G_1(y, q), G_2(y, q), ..., G_{n_2}(y, q))^T$, are also known. Here $u(x, y, \hat{p}, \hat{q})) = (u_1(x, y, \hat{p}, \hat{q})), u_2(x, y, \hat{p}, \hat{q})), ..., u_{n_2}(x, y, \hat{p}, \hat{q}))^T$ is the controller to be determined for the purpose of synchronizing the two identical or different chaotic(hyperchaotic) systems with fully unknown parameters p, q, and $\hat{p}$, $\hat{q}$ are the estimated values of parameters p, q. In this method $\hat{p}$, $\hat{q}$ are adapted duly by an adaptive control loop. $n_2 \leq n_1$ implies that the drive and response systems may have different dimensionality. Let the synchronization error of the two chaotic(hyperchaotic) systems be $e = (e_1, e_2, ..., e_{n_2})^T = (y_1 - x_1, y_2 - x_2, ..., y_{n_2} - x_{n_2}) \in R^{n_2}$. Then the error dynamical system between the drive system (1.21) and the response system (1.22) can be written as

$$\dot{e} = G(y, q) - F^*(x, p) + u(x, y, \hat{p}, \hat{q})), \tag{1.23}$$

where $F^*(x,p) = (F_1(x,p), F_2(x,p), ..., F_{n_2}(x,p))^T \in R^{n_2}$.

There is a method to find suitable feedback controller u and parameter update law of $\hat{p}$ and $\hat{q}$, such that the two chaotic(hyperchaotic) systems are identically synchronized. Let $\tilde{p} = \hat{p} - p, \tilde{q} = \hat{q} - q$ be the estimation errors of the parameters p and q. Construct a dynamical Lyapunov function consisting of the synchronization errors and the estimation errors of parameters

$$V(e, \hat{p}, \hat{q}) = \frac{1}{2} e^T P e + \frac{1}{2} \tilde{p}^T Q \tilde{p} + \frac{1}{2} \tilde{q}^T R q, \tag{1.24}$$

where $P \in R^{n2 \times n2}, Q \in R^{m1 \times m1}$ and $R \in R^{m2 \times m2}$ are positive definite constant matrices. One may choose P, Q,and R as the corresponding identity matrices in most cases.

The time derivative of V along the trajectories of (1.23) is

$$\frac{dV}{dt} = e^T P(G(y,q) - F^*(x,p) + u(x,y,\hat{p},\hat{q})) - (\tilde{p}^T Q \dot{\hat{p}} + \tilde{q}^T R \dot{\hat{q}}), \tag{1.25}$$

Suppose we are able to select appropriate controller $u(x,y,\hat{p},\hat{q})$ and parameters update law $\dot{\hat{p}}$ and $\dot{\hat{q}}$ such that dV/dt is negative definite. Then the Lyapunov stability theorem[101], ensures that the synchronization of chaotic(hyperchaotic) systems (1.21) and (1.22) is achieved under the chosen feedback controller u and the parameters update law $\dot{\hat{p}}, \dot{\hat{q}}$.

In chapter 3, we study FPS in Quantum-CNN oscillators through adaptive nonlinear control. Chapter 4 presents MFPS between hyperchaotic Chen and hyperchaotic Lü system through adaptive nonlinear control.

1.4.3 Open-Plus-Closed-Loop control method

Jackson and Grosu [104],[105], Chen and Dong [106] developed a powerful method of control: the open-plus-closed-loop (OPCL) method combining the advantages of the open-loop control with the closed-loop control. This method gives precise driving for any continuous system in order to reach any desired dynamics. The OPCL coupling was used earlier for CS in identical oscillators [104]-[109] and synchronization of identical complex networks [110]. The method has also been extended to mismatched systems[111],[112] to produce amplification or attenuation of chaos.

We briefly discuss the OPCL method for the synchronization of two chaotic systems. A chaotic or hyperchaotic driver is defined by

$$\dot{y} = f(y), y \epsilon R^n, \tag{1.26}$$

It drives another chaotic or hyperchaotic oscillator $\dot{x} = f(x), x \epsilon R^n$ to achieve a goal dynamics $g(t) = y(t)$. After coupling, the response system is given by

$$\dot{x} = f(x) + D(x, g), \tag{1.27}$$

where the coupling function is defined as

$$D(x, g) = \dot{g} - f(g) + (H - \frac{\partial f(g)}{\partial g})(x - g), \tag{1.28}$$

$\frac{\partial f(g)}{\partial g}$ is the Jacobian of the dynamical system and H is an arbitrary constant Hurwitz matrix $(n \times n)$ whose eigen values all have negative real parts. Rewriting $D(x, g) = D_1(x, g) + D_2(x, g)$, where $D_1(x, g) = \dot{g} - f(g)$ and $D_2(x, g) = (H - \frac{\partial f(g)}{\partial g})(x - g)$, it may be noted that $D_1(x, g)$ is an open-loop driving and $D_2(x, g)$ is a closed-loop(feedback) one. This is the reason for naming the method as OPCL method.

The error signal of the coupled system is defined by $e = x - g$ and $f(x)$ can be written using Taylor series expansion, as

$$f(x) = f(g) + \frac{\partial f(g)}{\partial g}(x - g) + \cdots . \tag{1.29}$$

Keeping the first-order terms in (1.29) and substituting in (1.27), the error dynamics is obtained as

$$\dot{e} = He \tag{1.30}$$

Since H is a Hurwitz matrix which has all its eigenvalues have negative real parts, $e \longrightarrow 0$ as $t \longrightarrow \infty$ and we obtain asymptotic synchronization.

FPS and MFPS in a few chaotic and hyperchaotic systems are studied through OPCL control method in chapters 5 and 6.

1.5 Solving nonlinear ODEs

Nonlinear systems are best described by a system of coupled nonlinear first order differential equations(ODEs). In most cases nonlinear ODEs can not be solved analytically and one has to resort to numerical methods. Several numerical schemes are available in the literature to solve given differential equations. The most widely used and simple algorithm is the Runge-Kutta fourth order method [113].

1.5.1 Runge-Kutta Fourth order method

Consider a system of ODEs of the form

$$\dot{\mathbf{x}} = \mathbf{F}(\mathbf{x}) \tag{1.31}$$

Let the value of $\mathbf{x}$ at time t_i is known and denote it as $\mathbf{x}_i$.Suppose we wish to calculate the value of $\mathbf{x}$ at time $t_{i+1} = t_i + h$, where h is the increment in time.The formulae for the fourth-order Runge-Kutta algorithm for (1.31) are

$$\begin{aligned}
\mathbf{k}_1 &= hF(\mathbf{x}_i) \\
\mathbf{k}_2 &= hF(\mathbf{x}_i + \mathbf{k}_1/2) \\
\mathbf{k}_3 &= hF(\mathbf{x}_i + \mathbf{k}_2/2) \\
\mathbf{k}_4 &= hF(x_i + \mathbf{k}_3) \\
t_{i+1} &= t_i + h \\
\mathbf{x}_{i+1} &= \mathbf{x}_i + \frac{1}{6}(\mathbf{k}_1 + 2\mathbf{k}_2 + 2\mathbf{k}_3 + \mathbf{k}_4)
\end{aligned}$$

Using the above step-by-step procedure the solution to (1.31) at any value of t can be approximated. The truncation error in the fourth-order algorithm is $O(h^5)$.

Chapter 2

Hybrid and Function projective synchronization in hyperchaotic Lü system through active nonlinear control

2.1 Introduction

In this chapter we study hybrid synchronization and FPS behaviour in hyperchaotic Lü system [119] by using active control method. It is believed that the chaotic systems with higher dimensional attractors like hyperchaotic systems have much wider applications. In fact, the presence of more than one positive Lyapunov exponent, clearly improves the security by generating more complex dyanmcis. Hyperchaos synchronization has recently become a subject of active research. The nonlinear active control method is simple, efficient and easy to implement in practical applications. We design active nonlinear controllers to obtain hybrid synchronization and FPS in two unidirectionally coupled identical hyperchotic Lü sytems.

2.2 Hyperchaotic Lü system

Lü system[117],[118] developed by Lü and Chen, connects the Lorenz and Chen attractors and represents the transition from one to the other. Recently, Chen et.al.,[119] proposed hyperchaotic Lü systembased on Lü system by introducing a

state feedback controller. The hyperchaotic Lü system is described by:

$$\begin{aligned} \dot{x} &= a(y-x)+w \\ \dot{y} &= -xz+cy \\ \dot{z} &= xy-bz \\ \dot{w} &= xz+rw \end{aligned} \tag{2.1}$$

where x, y, z and z are state variables and a, b, c are the parameters of Lü system and r is a control parameter. The analysis of the dynamics of the system, including the bifurcation diagram, Lyapunov exponent spectrum and Poincare mapping and electronic circuit simulation experiments confirm the hyperchaotic nature of the system.

When $a = 36, b = 3, c = 20, -0.35 \leq r \leq 1.3$, system (2.1) is hyperchaotic. The chaotic attractor for the Lü hyperchaotic system is shown in Fig.2.1.

2.3 Hybrid synchronization of hyperchaotic Lü system

Recently, Li[59] studied hybrid synchronization behaviour in chaotic systems. In hybrid synchronization scheme, one part of the system is anti-synchronized and the other completely synchronized so that complete synchronization (CS) and anti-synchronization (AS) co-exist in the system. The co-existence of CS and AS enhances security in communication and chaotic encryption schemes. In this section we study the hybrid synchronization behaviour in hyperchotic Lü system using active nonlinear control method. We design active controllers so that two pairs of states are synchronized and the other two pairs are anti-synchronized.

In order to observe the hybrid synchronizaton behaviour in the Lü hyperchaotic system, we have two Lü hyperchaotic systems where the drive system with the four state variables denoted by subscript 1 drives the response system having identical equations denoted by the subscript 2. However, the initial condition on the drive system is different from that of the response system. The two Lü systems are described by the following equations.

$$\begin{aligned} \dot{x}_1 &= a(y_1-x_1)+w_1 \\ \dot{y}_1 &= -x_1z_1+cy_1 \\ \dot{z}_1 &= x_1y_1-bz_1 \\ \dot{w}_1 &= x_1z_1+rw_1 \end{aligned} \tag{2.2}$$

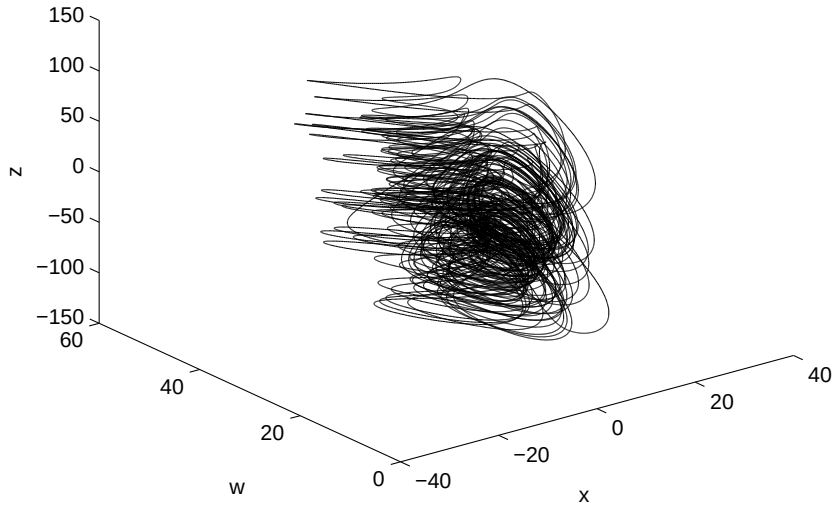

(a)

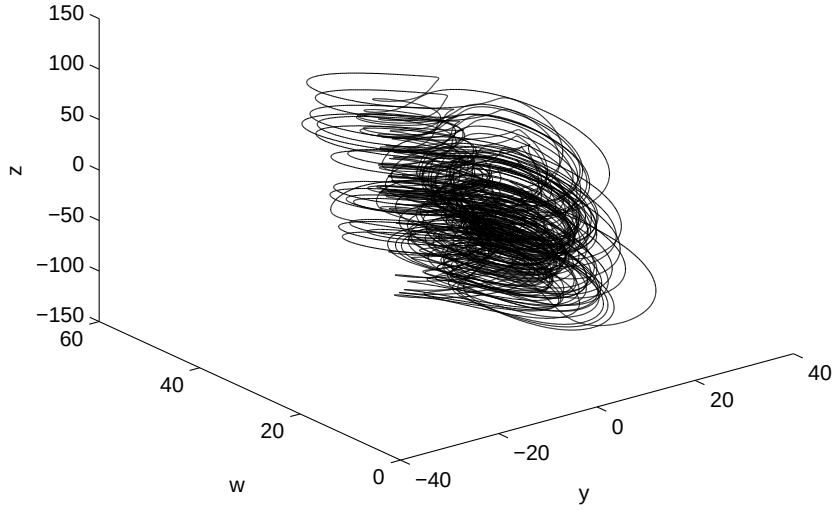

(b)

Figure 2.1: The chaotic attractor for Lü hyperchaotic system.

and

$$\begin{aligned}\dot{x}_2 &= a(y_2 - x_2) + w_2 + u_1\\ \dot{y}_2 &= -x_2 z_2 + c y_2 + u_2\\ \dot{z}_2 &= x_2 y_2 - b z_2 + u_3\\ \dot{w}_2 &= x_2 z_2 + r w_2 + u_4\end{aligned} \tag{2.3}$$

We have introduced four active control functions $u_1(t), u_2(t), u_3(t)$ and $u_4(t)$. These control functions are to be determined for the purpose of hybrid synchronization of the two systems with the same parameters and different initial conditions.

For the hybrid synchronization, we define the state errors between the response system that is to be controlled and the controlling drive system as

$$\begin{aligned}e_1 &= x_2 - x_1\\ e_2 &= y_2 + y_1\\ e_3 &= z_2 - z_1\\ e_4 &= w_2 + w_1\end{aligned} \tag{2.4}$$

Then the error dynamical system is obtained as

$$\begin{aligned}\dot{e}_1 &= -a e_1 + a e_2 + e_4 - 2a y_1 - 2 w_1 + u_1\\ \dot{e}_2 &= c e_2 - x_2 z_2 - x_1 z_1 + u_2\\ \dot{e}_3 &= -b e_3 + x_2 y_2 - x_1 y_1 + u_3\\ \dot{e}_4 &= r e_4 + x_2 z_2 + x_1 z_1 + u_4\end{aligned} \tag{2.5}$$

We redefine the active control function $u = [u_1(t), u_2(t), u_3(t), u_4(t)]^T$ as

$$\begin{aligned}u_1(t) &= 2a y_1 + 2 w_1 + v_1(t)\\ u_2(t) &= x_2 z_2 + x_1 z_1 + v_2(t)\\ u_3(t) &= -x_2 y_2 + x_1 y_1 + v_3(t)\\ u_4(t) &= -x_2 z_2 - x_1 z_1 + v_4(t)\end{aligned} \tag{2.6}$$

Substituting (2.6) in (2.5) gives

$$\begin{aligned}\dot{e}_1 &= -a e_1 + a e_2 + e_4 + v_1(t)\\ \dot{e}_2 &= c e_2 + v_2(t)\\ \dot{e}_3 &= -b e_3 + v_3(t)\\ \dot{e}_4 &= r e_4 + v_4(t)\end{aligned} \tag{2.7}$$

Thus, the system (2.7) to be controlled is a linear system with the control input function $v = [v_1(t), v_2(t), v_3(t), v_4(t)]^T$ as functions of the error states e_1, e_2, e_3 and e_4. When (2.7) is stabilized by the feedback v, the error will converge to zero as

$t \to \infty$ which implying that the system (2.2) and (2.3) get globally synchronized. To achieve this goal, we choose v as

$$[v_1(t), v_2(t), v_3(t), v_4(t)]^T = A[e_1(t), e_2(t), e_3(t), e_4(t)]^T \tag{2.8}$$

where A is a 4×4 matrix. For (2.7) to be asymptotically stable, the elements of the matrix A are properly chosen so that the closed loop system(2.7) will have all eigenvalues with negative real parts. Various choices of A are possible. A good choice is

$$A = \begin{bmatrix} (a-1) & -a & 0 & -1 \\ 0 & -(c+1) & 0 & 0 \\ 0 & 0 & b-1 & 0 \\ 0 & 0 & 0 & -(r+1) \end{bmatrix} \tag{2.9}$$

In this particular choice, the closed loop system (2.7) has eigenvalues $\lambda_1 = -1, \lambda_2 = -1, \lambda_3 = -1$and $\lambda_4 = -1$.

Hence the error system becomes

$$\begin{aligned} \dot{e}_1 &= -e_1 \\ \dot{e}_2 &= -e_2 \\ \dot{e}_3 &= -e_3 \\ \dot{e}_4 &= -e_4 \end{aligned} \tag{2.10}$$

Obviously the error states e_1, e_2, e_3 and e_4 converge to zero as time t tends to infinity.

Alternatively we can show that hybrid synchronization is achieved through the application of the designed active nonlinear controls using the Lyapunov stability theorem.

Theorem.*Systems (2.2) and (2.3) can be exponentially and globally hybrid synchronized for any initial condition with the active nonlinear controllers (2.6).*

Proof. We choose Lyapunov function as follows

$$V(t) = \frac{1}{2}(e_1^2 + e_2^2 + e_3^2 + e_4^2) \tag{2.11}$$

By using the control law, the time derivative of $V(t)$ along trajectories (2.5) can be derived as $\dot{V}(t) = e_1\dot{e}_1 + e_2\dot{e}_2 + e_3\dot{e}_3 + e_4\dot{e}_4$

$= e_1(-e_1) + e_2(-e_2) + e_3(-e_3) + e_4(-e_4)$

$= -e_1^2 - e_2^2 - e_3^2 - e_4^2$

≤ 0 which by Lyapunov's theorem implies that $e_i = 0 (i = 1, 2, 3, 4)$ as $t \to \infty$ and guarantees the exponentially asymptotical stability of the error system (2.5).

Therefore, system (2.2) and (2.3) can achieve exponentially asymptotical hybrid synchronization for any initial condition with active nonlinear controllers (2.6).

2.4 Simulation results

Numerical simulations are performed using the fourth order Runge-Kutta integration method to solve the two systems of differential equations (2.2) and (2.3) with time step size equal to 0.001. We select the parameters of the Lü hyperchaotic system as $a = 36, b = 3, c = 20, r = 1.3$ so that the Lü system exhibits hyperchaotic behaviour. The initial values for the drive and response systems are $x_1(0) = 5, y_1(0) = 8, z_1(0) = -1, w_1(0) = -3$ and $x_2(0) = 3, y_2(0) = 4, z_2(0) = 5, w_2(0) = 5$ respectively. Fig. 2.2 and 2.3 shows the time response of states x_1, y_1, z_1 and w_1 for the drive system (2.2) and the states x_2, y_2, z_2 and w_2 for the response system (2.3) under the application of active control where control is applied after 10 units of time. Fig. 2.4 displays the time response of the error system (2.4).

2.5 Function projective synchronization of hyperchaotic Lü system

Consider the following master and slave system

$$\dot{\mathbf{x}} = \mathbf{f}(\mathbf{x}) \tag{2.12}$$

$$\dot{\mathbf{y}} = \mathbf{g}(\mathbf{y}) + \mathbf{u}(\mathbf{x}, \mathbf{y}) \tag{2.13}$$

where $\mathbf{x}, \mathbf{y} \in \mathbf{R}^n$ are the state vectors, $\mathbf{f}, \mathbf{g} : \mathbf{R}^n \to \mathbf{R}^n$ are continuous nonlinear vector functions, $\mathbf{u}(\mathbf{x}, \mathbf{y})$ is the vector controller. We define the error system as

$$\mathbf{e}(\mathbf{t}) = \mathbf{y} - \alpha(t)\mathbf{x}$$

where $\alpha(t)$ is a continuously differentiable function with $\alpha(t) \neq 0$ for all t.

The system (2.12) and (2.13) are said to be in FPS, if there exists a scaling function $\alpha(t)$ such that $\lim_{t\to\infty} \|\mathbf{e}(t)\| = 0$.

For the FPS, we define the state errors between the response system (2.3) that

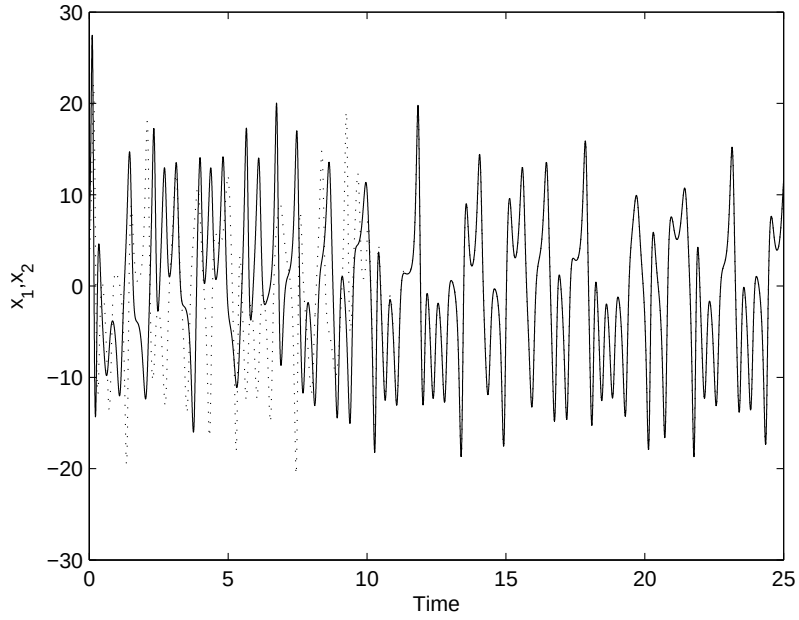

(a)

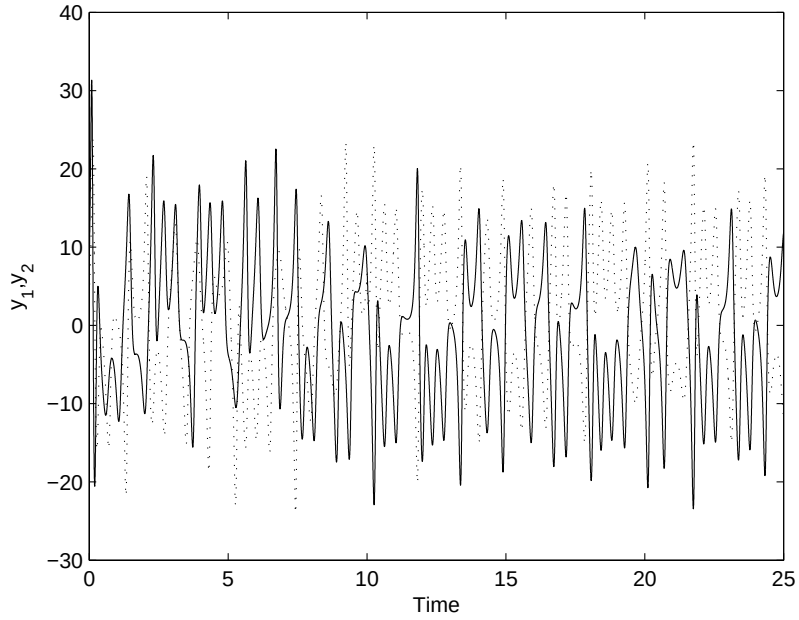

(b)

Figure 2.2: Drive and response system states when control is activated after 10 units of time (a)time series of x_1(solid line) and x_2(dotted line)(b)time series of y_1(solid line) and y_2(dotted line)

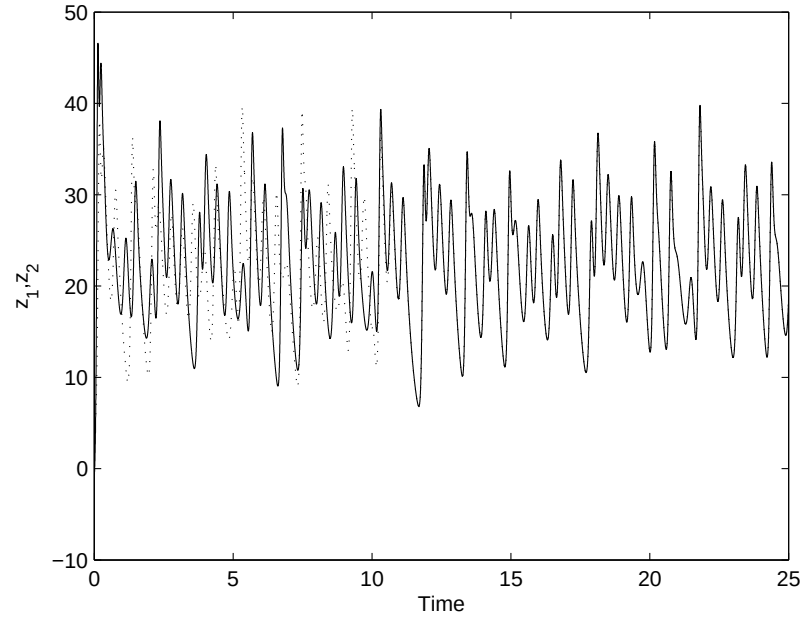

(a)

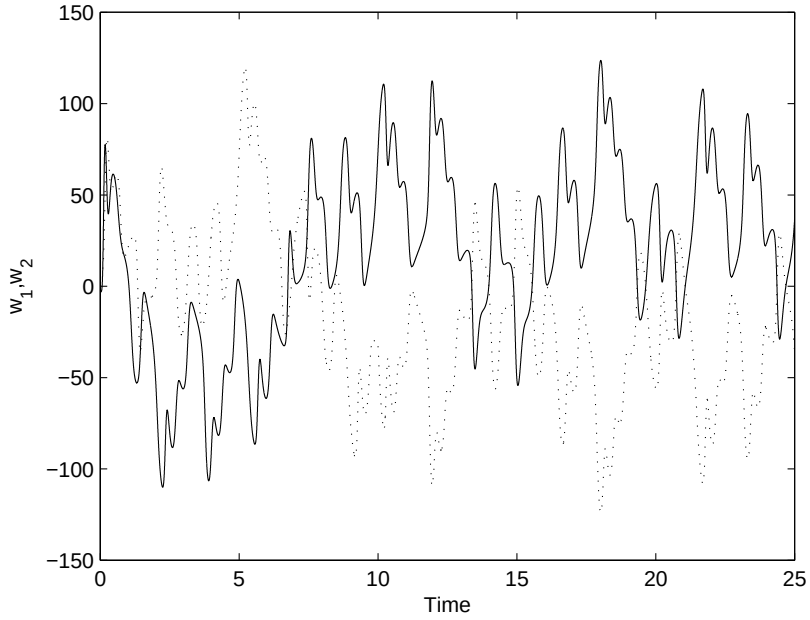

(b)

Figure 2.3: Drive and response system states when control is activated after 10 units of time (a)time series of z_1(solid line) and z_2(dotted line)(b)time series of w_1(solid line) and w_2(dotted line)

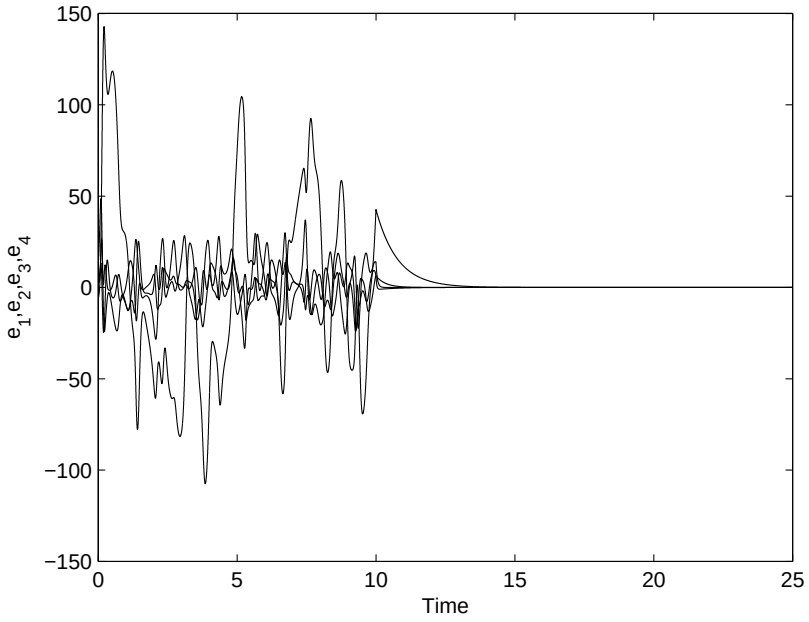

Figure 2.4: Hybrid synchronization error signals between drive and response system when control is applied after 10 units of time

is to be controlled and the controlling drive system (2.2) as

$$\begin{aligned} e_1 &= x_2 - \alpha(t)x_1 \\ e_2 &= y_2 - \alpha(t)y_1 \\ e_3 &= z_2 - \alpha(t)z_1 \\ e_4 &= w_2 - \alpha(t)w_1 \end{aligned} \tag{2.14}$$

The error dynamics of the system is obtained as:

$$\begin{aligned} \dot{e}_1 &= -ae_1 + ae_2 + e_4 - \dot{\alpha}(t)x_1 + u_1 \\ \dot{e}_2 &= ce_2 - x_2z_2 + \alpha(t)x_1z_1 - \dot{\alpha}(t)y_1 + u_2 \\ \dot{e}_3 &= -be_3 + x_2y_2 - \alpha(t)x_1y_1 - \dot{\alpha}(t)z_1 + u_3 \\ \dot{e}_4 &= re_4 + x_2z_2 - \alpha(t)x_1z_1 - \dot{\alpha}(t)w_1 + u_4 \end{aligned} \tag{2.15}$$

Let us redefine the active control function $u = [u_1(t), u_2(t), u_3(t), u_4(t)]^T$ as

$$\begin{aligned} u_1(t) &= \dot{\alpha}(t)x_1 + v_1(t) \\ u_2(t) &= x_2z_2 - \alpha(t)x_1z_1 + \dot{\alpha}(t)y_1 + v_2(t) \\ u_3(t) &= -x_2y_2 + \alpha(t)x_1y_1 + \dot{\alpha}(t)z_1 + v_3(t) \\ u_4(t) &= -x_2z_2 + \alpha(t)x_1z_1 + \dot{\alpha}(t)w_1 + v_4(t) \end{aligned} \tag{2.16}$$

where $v_i(t)$ are to be determined.

Substitution of (2.16) in (2.15) gives

$$\begin{aligned} \dot{e}_1 &= -ae_1 + ae_2 + e_4 + v_1(t) \\ \dot{e}_2 &= ce_2 + v_2(t) \\ \dot{e}_3 &= -be_3 + v_3(t) \\ \dot{e}_4 &= re_4 + v_4(t) \end{aligned} \tag{2.17}$$

Thus, the system (2.17) to be controlled is a linear system with the control input function $v = [v_1(t), v_2(t), v_3(t), v_4(t)]^T$ as functions of the error states e_1, e_2, e_3 and e_4. When (2.17) is stabilized by the feedback v, the error will converge to zero as $t \to \infty$ which implies that the system (2.2) and (2.3) are globally function projective synchronized. To achieve this goal, we choose v such that

$$[v_1(t), v_2(t), v_3(t), v_4(t)]^T = A[e_1(t), e_2(t), e_3(t), e_4(t)]^T \tag{2.18}$$

where A is a constant 4×4 matrix. For (2.17) to be asymptotically stable, the elements of the matrix A are properly chosen so that the closed loop system(2.17) will have all eigenvalues with negative real parts. Various choices of A are possible. A good choice is

$$A = \begin{bmatrix} (a-1) & -a & 0 & -1 \\ 0 & -(c+1) & 0 & 0 \\ 0 & 0 & b-1 & 0 \\ 0 & 0 & 0 & -(r+1) \end{bmatrix} \tag{2.19}$$

With this particular choice, the closed loop system (2.17) will have the eigenvalues $\lambda_1 = -1, \lambda_2 = -1, \lambda_3 = -1$and $\lambda_4 = -1$.

Hence the error system becomes

$$\begin{aligned} \dot{e}_1 &= -e_1 \\ \dot{e}_2 &= -e_2 \\ \dot{e}_3 &= -e_3 \\ \dot{e}_4 &= -e_4 \end{aligned} \tag{2.20}$$

Thus the error states e_1, e_2, e_3 and e_4 converge to zero as time t tends to infinity.

An alternative proof of the attaintment of FPS through the application of designed active nonlinear control can be given using the Lypunov stability theorem.

Theorem.*Systems (2.2) and (2.3) can be exponentially and globally function projective synchronized for any initial condition with the active nonlinear controllers*

(2.16).

Proof. We choose Lyapunov function as follows

$$V(t) = \frac{1}{2}(e_1^2 + e_2^2 + e_3^2 + e_4^2) \tag{2.21}$$

By using the control law, the time derivative of along trajectories (2.15) can be derived as

$$\begin{aligned}\dot{V}(t) &= e_1\dot{e}_1 + e_2\dot{e}_2 + e_3\dot{e}_3 + e_4\dot{e}_4 \\ &= e_1(-e_1) + e_2(-e_2) + e_3(-e_3) + e_4(-e_4) \\ &= -e_1^2 - e_2^2 - e_3^2 - e_4^2 \\ &\leq 0\end{aligned}$$

which implies that $e_i = 0(i = 1, 2, 3, 4)$ as $t \to \infty$ and guarantees the exponentially asymptotical stability of the error system (2.15). Therefore, system (2.2) and (2.3) can achieve exponentially asymptotical FPS for any initial condition with active nonlinear controllers (2.16).

2.6 Simulation results

In simulations, the fourth order Runge-Kutta integration method is used to solve the two systems of differential equations (2.2) and (2.3) with time step size equal to 0.001. We select the parameters of the Lü hyperchaotic system as $a = 36, b = 3, c = 20, r = 1.3$ so that the Lü system exhibits hyperchaotic behaviour. The initial values for the drive and response systems are $x_1(0) = 5, y_1(0) = 8, z_1(0) = -1, w_1(0) = -3$ and $x_2(0) = 3, y_2(0) = 4, z_2(0) = 5, w_2(0) = 5$ respectively. The scaling function is chosen as $\alpha(t) = 1 + 0.5sin(2\pi t/20)$. Fig. 2.5 and 2.6 shows the time response of states x_1, y_1, z_1 and w_1 for the drive system (2.2) and the states x_2, y_2, z_2 and w_2 for the response system (2.3) under the application of active control. Fig. 2.7 displays the time response of the error system (2.14). In fig.2.8 is given the ratio r_r/r_d, where $r_r = \sqrt{x_2^2 + y_2^2 + z_2^2 + w_2^2}$ and $r_d = \sqrt{x_1^2 + y_1^2 + z_1^2 + w_1^2}$ showing that it tends to the scaling function.

Obviously, the synchronization errors coverage to zero with exponentially asymptotical speed and two systems with different initial values achieve FPS very quickly.

2.7 Conclusions

This work demonstrates that hybrid synchronization and FPS between two identical Lü hyperchaotic systems can be achieved through active control method. Appropriate controls are designed through active nonlinear control theory for the desired

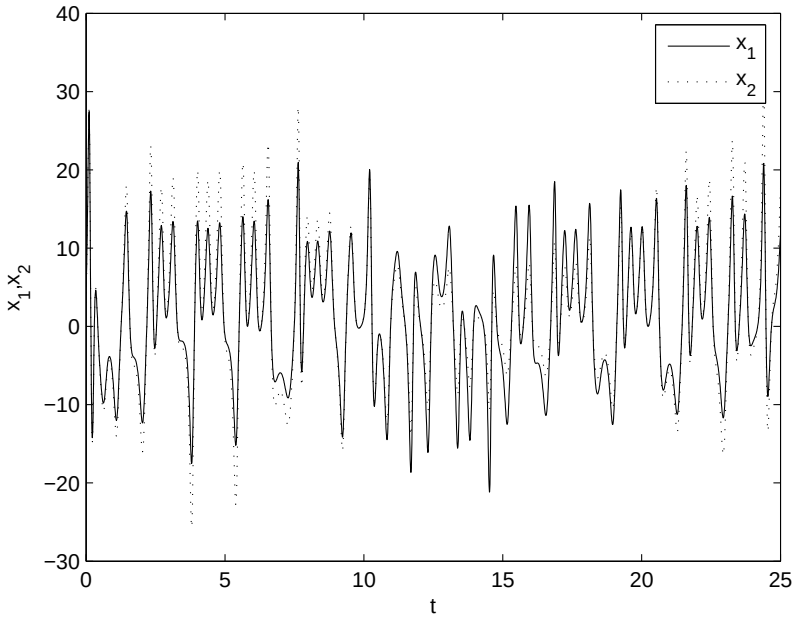

(a)

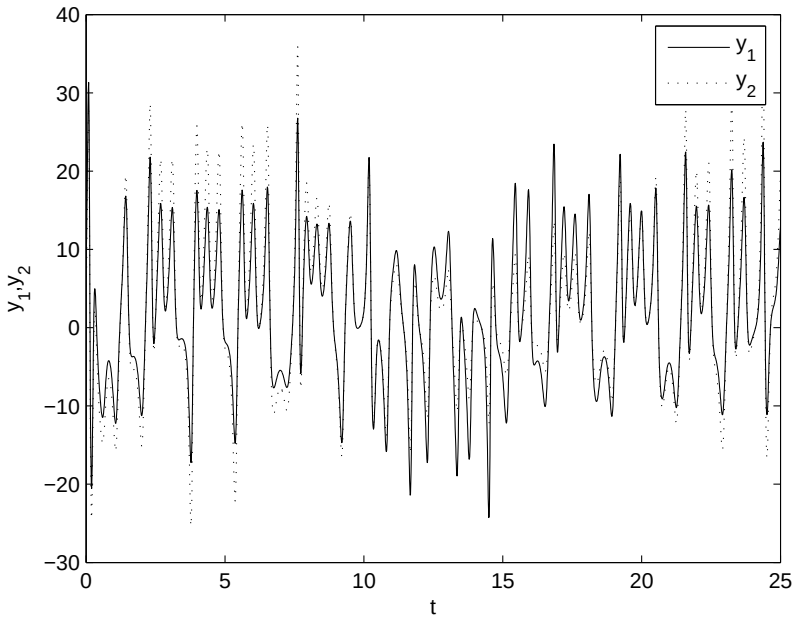

(b)

Figure 2.5: (a)time series of x_1(solid line) and x_2(dotted line)(b)time series of y_1(solid line) and y_2(dotted line

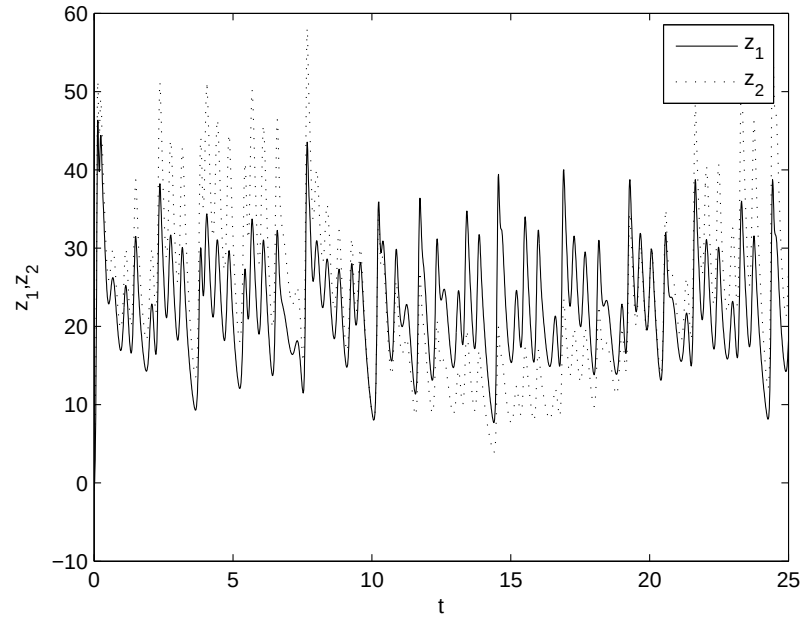

(a)

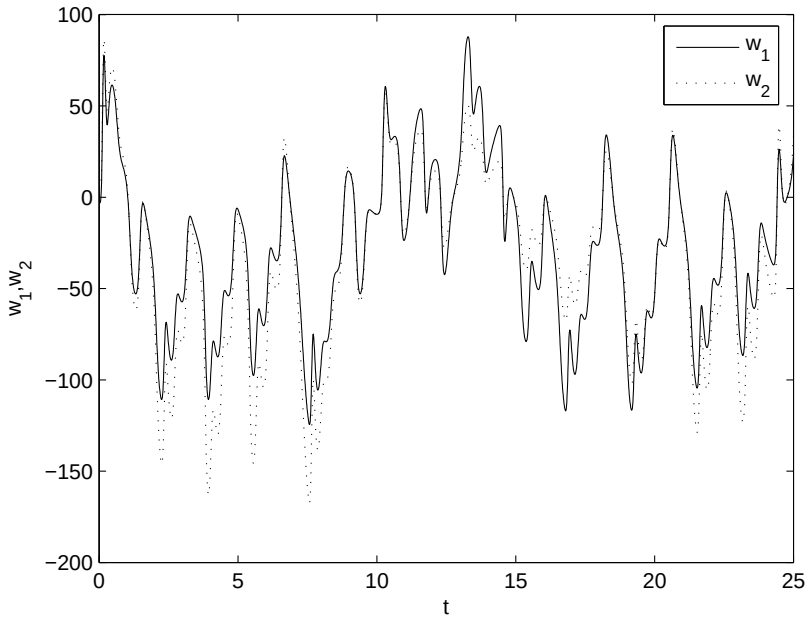

(b)

Figure 2.6: (a)time series of z_1(solid line) and z_2(dotted line)(b)time series of w_1(solid line) and w_2(dotted line)

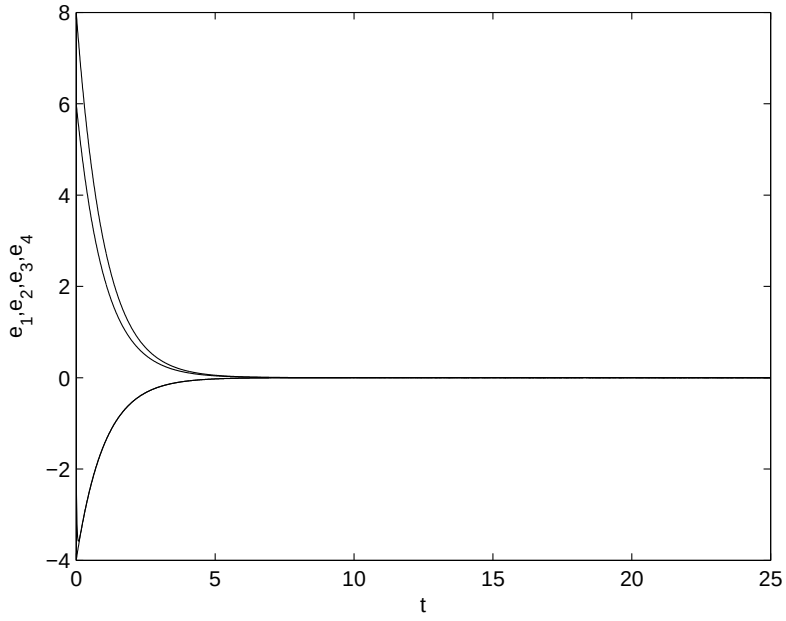

Figure 2.7: Function projective synchronization error signals between drive and response system

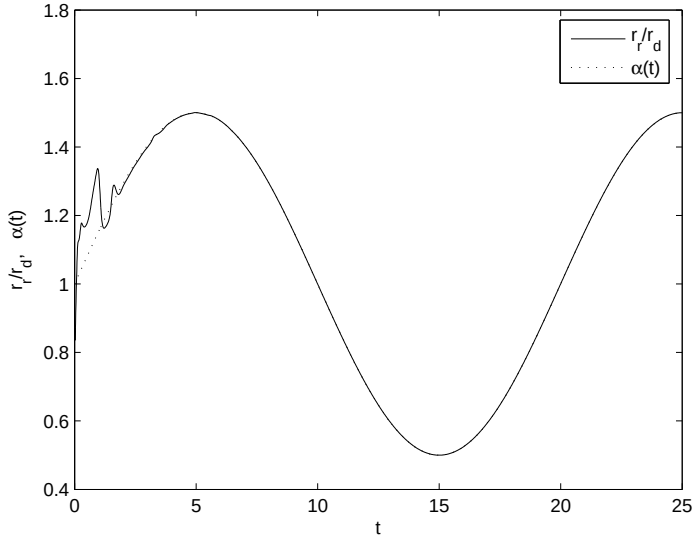

Figure 2.8: Variation of the ratio r_r/r_d and the scaling function $\alpha(t)$

synchronization behaviour. Under the application of control the slave system displays hybrid synchronization and FPS behaviour with respect to the drive system. Numerical simulations verify the effectiveness of the proposed control techniques.

Chapter 3

Function projective synchronization of two-cell Quantum-CNN oscillator through adaptive nonlinear control

3.1 Introduction

In this chapter we investigate FPS of recently developed two-cell Quantum-CNN(Cellular Nonlinear Network) oscillators. Recently, Q-CNN oscillators have attracted attention of scientists and engineers as a nano scale chaos generator[114]. We consider two hyperchaotic Quantum-CNN oscillators coupled in unidirectional fashion. The parameters of the response system are assumed to be unknown. Based on adaptive control theory we design adaptive nonlinear controls and parameter estimation rules to obtain FPS under parameter uncertainity of the response system.

3.2 Quantum-CNN oscillator

In the last decade much attention has been devoted to quantum dots and quantum dots cellular automata (QCA) with particular orientation towards quantum computing . A quantum dot is an "artificial atom" obtained by including a small quantity of material in a substrate. Four dots realized on the same layer constitute a QCA cell. In each cell two extra electrons can assume different locations by tunneling between

the dots and providing the cell with a certain polarization. The expectation values ρ_i of the charge on each dot define the polarization P of the cells and due to superposed states, P can vary continuously between -1 and $+1$. The polarization constitutes the macroscopic degree of freedom of the cell and therefore it can be assumed as a state variable. Considering quantum phase displacement ϕ as microscopic degree of freedom, with the help of Schrödinger equation, we can obtain following equation for a QCA cell.

$$\begin{aligned} i\hbar\frac{\partial}{\partial t}P_k &= -2\gamma\sqrt{1-P_k^2}\sin\phi_k \\ i\hbar\frac{\partial}{\partial t}\phi_k &= -\overline{P}_k E_k + 2\gamma\frac{P_k}{\sqrt{1-P_k^2}}\cos\phi_k \end{aligned} \tag{3.1}$$

where γ is the interdot tunneling energy, takes into account the neighboring polarizations and E_k is the electrostatic energy cost of two adjacent fully polarized cells having opposite polarization. The effect of local interconnections is taken into account in the term $\overline{P}_k$.

With appropriate transformations, for a two-cell Quantum-CNN, following differential equations are obtained [114]

$$\begin{aligned} \dot{x}_1 &= -2a\sqrt{1-x_1^2}\sin x_2 \\ \dot{x}_2 &= -c(x_1-x_3) + 2a\frac{x_1}{\sqrt{1-x_1^2}}\cos x_2 \\ \dot{x}_3 &= -2b\sqrt{1-x_3^2}\sin x_4 \\ \dot{x}_4 &= -d(x_3-x_1) + 2b\frac{x_3}{\sqrt{1-x_3^2}}\cos x_4 \end{aligned} \tag{3.2}$$

where x_1 and x_3 are polarizations, x_2 and x_4 are quantum phase displacements, a and b are proportional to the inter-dot energy inside each cell and c and d are the parameters that weigh the effects on the cell of the difference of polarizations of the neighbouring cells. The system exhibits hyperchaotic behaviour for a range of parameter values[115]. The hyperchaotic attractor of the system when $a = 19.4$, $b = 13.1$, $c = 9.529$ and $d = 7.94$, is shown in figure 3.1 and 3.2.

3.3 Adaptive Function projective synchronization

Consider a class of uncertain chaotic system described by

$$\dot{x} = f(x) + F(x)\theta, \tag{3.3}$$

where $x \in \mathbf{R}^n$ is the state vector of the system, $\mathbf{f} : \mathbf{R}^n \to \mathbf{R}^n$ is a continuous

vector function, $\mathbf{F} : \mathbf{R}^n \rightarrow \mathbf{R}^n$ is a function matrix, $\theta \in \mathbf{R}^p$ is an unknown parameter vector.

Assuming the system (3.3) be the drive system, the controlled response system can be taken as

$$\dot{y} = f(y) + F(y)\hat{\theta} + u \tag{3.4}$$

where $y \in \mathbf{R}^n$ is the state vector of the system, $\hat{\theta} \in \mathbf{R}^p$ represents the estimate parameter vector of unknown parameters of the slave system, $u \in R^n$ is a controller to be determined. The FPS error is defined as $e = y - \alpha(t)x$. The goal of control is to find out an appropriate u such that the response system is in FPS with the drive system and the unknown parameters are identified simultaneously.

The error dynamical system between the drive system (3.3) and the response system(3.4) is

$$\begin{aligned} \dot{e} &= \dot{y} - \alpha(t)\dot{x} - \dot{\alpha}(t)x \\ &= f(y) + F(y)\hat{\theta} + u - \alpha(t)f(x) - \alpha(t)F(x)\theta - \dot{\alpha}(t)x \end{aligned} \tag{3.5}$$

Let us choose the controllers of the form

$$u = -f(y) + \alpha(t)f(x) - (F(y) - \alpha(t)F(x))\hat{\theta} + \dot{\alpha}(t)x - ke \tag{3.6}$$

and the parameter update rule

$$\dot{\hat{\theta}} = -F(x)^T\alpha(t)e - l\tilde{\theta} \tag{3.7}$$

where $\tilde{\theta} = \hat{\theta} - \theta$ and $k = diag(k_1, k_2, ..., k_n)$ and $l = diag(l_1, l_2, ..., l_p)$ are constant positive matrices.

Substituting for u in (3.5) from (3.6), the error dynamics is described by

$$\dot{e} = \alpha(t)F(x)\widetilde{\theta} - ke \tag{3.8}$$

Consequently, the FPS problem becomes the stability of error dynamics (3.8) and (3.7). If it is globally stabilized at the origin, the FPS of the drive system (3.3) and the response system(3.4) can be globally realized.

Theorem. *For the given scaling function $\alpha(t)$, the function projective synchronization between drive system(3.3) and response system(3.4) will occur by the control law(3.6) and the parameter update rule(3.7)*

Proof: Choose the following Lyapunov function

$$V = \frac{1}{2}[e^T e + \overset{\sim}{\theta}^T \overset{\sim}{\theta}] \tag{3.9}$$

With the controllers (3.6) and the parameter update rule (3.7), the time derivative of the Lyapunov function along the trajectory of error system (3.8) and (3.7) is

$$\begin{aligned} \dot{V} &= e^T \dot{e} + \overset{\sim}{\theta}^T \dot{\overset{\sim}{\theta}} \\ &= e^T(\alpha(t)F(x)\overset{\sim}{\theta} - ke) + \overset{\sim}{\theta}^T(-F(x)^T\alpha(t)e - l\overset{\sim}{\theta}) \\ &= -e^T ke - \overset{\sim}{\theta}^T l\overset{\sim}{\theta} < 0 \end{aligned}$$

Therefore according to the Lyapunov stability theorem, the origin is stable and adaptive FPS of (3.3) and (3.4) is obtained.

3.4 Adaptive FPS of two-cell Quantum-CNN oscillators

We assume that we have two Quantum-CNN oscillators where the master system (3.2) drives the slave system (3.10)

$$\begin{aligned} \dot{y}_1 &= -2a_1\sqrt{1-y_1^2}\sin y_2 + u_1 \\ \dot{y}_2 &= -c_1(y_1 - y_3) + 2a_1\tfrac{y_1}{\sqrt{1-y_1^2}}\cos y_2 + u_2 \\ \dot{y}_3 &= -2b_1\sqrt{1-y_3^2}\sin y_4 + u_3 \\ \dot{y}_4 &= -d_1(y_3 - y_1) + 2b_1\tfrac{y_3}{\sqrt{1-y_3^2}}\cos y_4 + u_4 \end{aligned} \tag{3.10}$$

where a_1, b_1, c_1 and d_1 are the estimate parameters of the slave system and u_1, u_2, u_3 and u_4 are the nonlinear controllers such that two chaotic systems can be in FPS. For (3.2), $f(x) = 0$ and

$$F(x) = \begin{bmatrix} -2\sqrt{1-x_1^2}\sin x_2 & 0 & 0 & 0 \\ 2\frac{x_1}{\sqrt{1-x_1^2}}\cos x_2 & 0 & -(x_1 - x_3) & 0 \\ 0 & -2\sqrt{1-x_3^2}\sin x_4 & 0 & 0 \\ 0 & 2\frac{x_3}{\sqrt{1-x_3^2}}\cos x_4 & 0 & -(x_3 - x_1) \end{bmatrix}.$$

Then, according to (3.6) and (3.7) we get the following controller

$$\begin{aligned}
u_1 &= 2a_1(\sqrt{1-y_1^2}\sin y_2 - \alpha(t)\sqrt{1-x_1^2}\sin x_2) + \dot{\alpha}(t)x_1 - k_1e_1 \\
u_2 &= c_1((y_1-y_3) - \alpha(t)(x_1-x_2)) \\
&\quad -2a_1(\tfrac{y_1}{\sqrt{1-y_1^2}}\cos y_2 - \alpha(t)\tfrac{x_1}{\sqrt{1-x_1^2}}\cos x_2) + \dot{\alpha}(t)x_2 - k_2e_2 \\
u_3 &= 2b_1(\sqrt{1-y_3^2}\sin y_4 - \alpha(t)\sqrt{1-x_3^2}\sin x_4) + \dot{\alpha}(t)x_3 - k_3e_3 \\
u_4 &= d_1((y_3-y_1) - \alpha(t)(x_3-x_1)) \\
&\quad -2b_1(\tfrac{y_3}{\sqrt{1-y_3^2}}\cos y_4 - \alpha(t)\tfrac{x_3}{\sqrt{1-x_3^2}}\cos x_4) + \dot{\alpha}(t)x_4 - k_4e_4
\end{aligned} \tag{3.11}$$

and the update rule for the four unknown parameters a_1, b_1, c_1 and d_1 are

$$\begin{aligned}
\dot{a}_1 &= 2\alpha(t)(\sqrt{1-x_1^2}\sin x_2e_1 - \tfrac{x_1}{\sqrt{1-x_1^2}}\cos x_2e_2) - l_1(a_1-a) \\
\dot{b}_1 &= 2\alpha(t)(\sqrt{1-x_3^2}\sin x_4e_3 - \tfrac{x_3}{\sqrt{1-x_3^2}}\cos x_4e_4) - l_2(b_1-b) \\
\dot{c}_1 &= \alpha(t)(x_1-x_3)e_2 - l_3(c_1-c) \\
\dot{d}_1 &= \alpha(t)(x_3-x_1)e_4 - l_4(d_1-d)
\end{aligned} \tag{3.12}$$

3.5 Numerical simulations

In this section, numerical simulations are presented to verify the effectiveness of the proposed synchronization controller. Fourth-order Runge-Kutta method is used to solve systems(3.2)and(3.10) with time step size 0.001. The parameters are chosen to be $a = 19.4$, $b = 13.1$, $c = 9.529$ and $d = 7.94$, so that the Quantum-CNN oscillator has chaotic attractor. The initial conditions of the drive system are $x_1(0) = 0.55, x_2(0) = -0.1, x_3(0) = -0.4$ and $x_4(0) = 0.5$, and those of the response system are $y_1(0) = -0.6, y_2(0) = 0.25, y_3(0) = 0.5$ and $y_4(0) = 0.3$. Moreover the initial values of the estimated parameters are chosen as $a_1(0) = 2$, $b_1(0) = 15$, $c_1(0) = 0$ and $d_1(0) = 9$ and the scaling function is chosen as $\alpha(t) = 0.5 + 0.1\sin(t)$. Furthermore, the control gains are chosen as $(k_1, k_2, k_3, k_4) = (0.5, 0.5, 0.5, 0.5)$ and $(l_1, l_2, l_3, l_4) = (0.5, 0.5, 0.5, 0.5)$. The simulation results are illustrated in Figs. 3.3 ,3.4 and 3.5. Fig. 3.3 shows the error variables e_1, e_2, e_3, e_4 tend to zero for large t. Fig.3.4 shows that the estimated values of the unknown parameters converge to $a = 19.4$, $b = 13.1$, $c = 9.529$ and $d = 7.94$ as $t \longrightarrow \infty$, respectively. Fig.3.5 displays the ratio r_r/r_d, where $r_r = \|y\|$ and $r_d = \|x\|$ and shows that it tends to the predefined scaling function $\alpha(t)$.

3.6 Conclusion

This work investigated the FPS of two-cell Quantum-CNN oscillators. Based on Lyapunov stability theory, we design adaptive synchronization controllers with corresponding parameter update laws to synchronize the two systems. All the theoretical results are verified by numerical simulations to demonstrate the effectiveness of the proposed synchronization scheme.

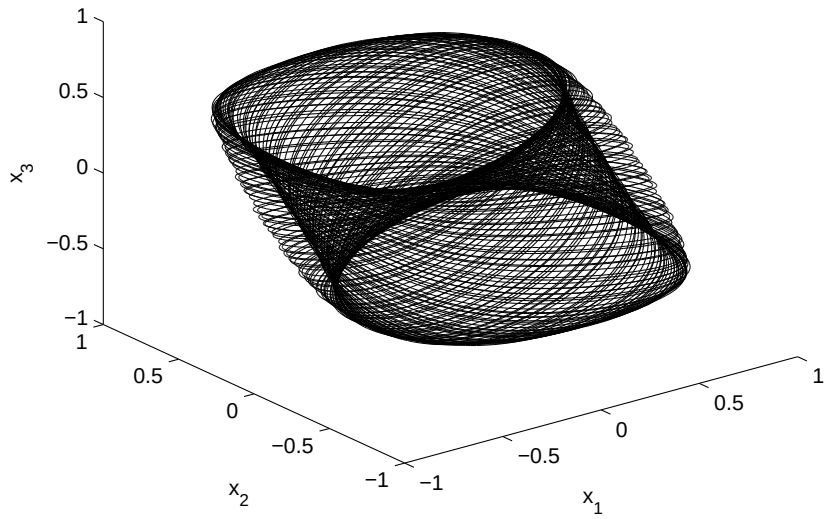

(a)

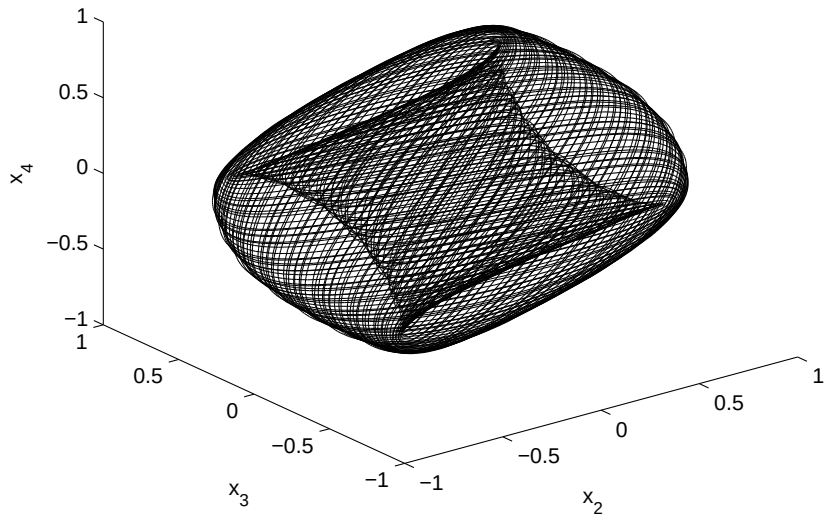

(b)

Figure 3.1: Chaotic attractor of Quantum-CNN system (a) in (x_1, x_2, x_3) space(b)in (x_2, x_3, x_4) space

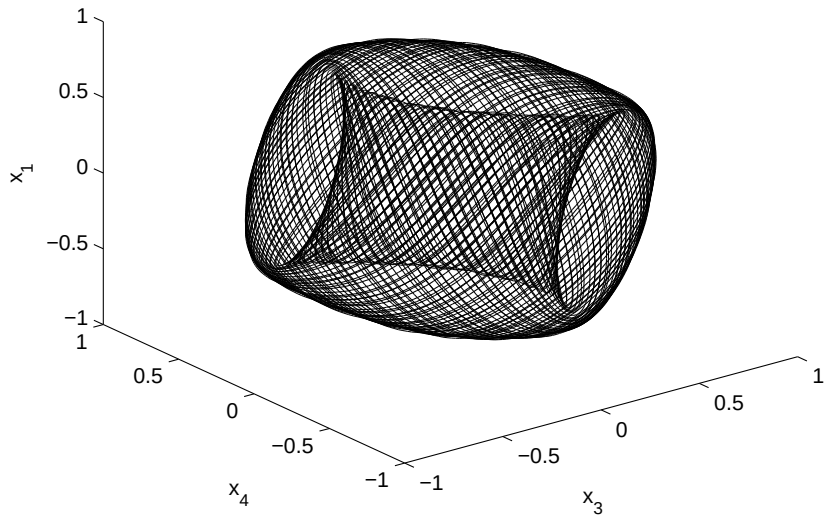

(a)

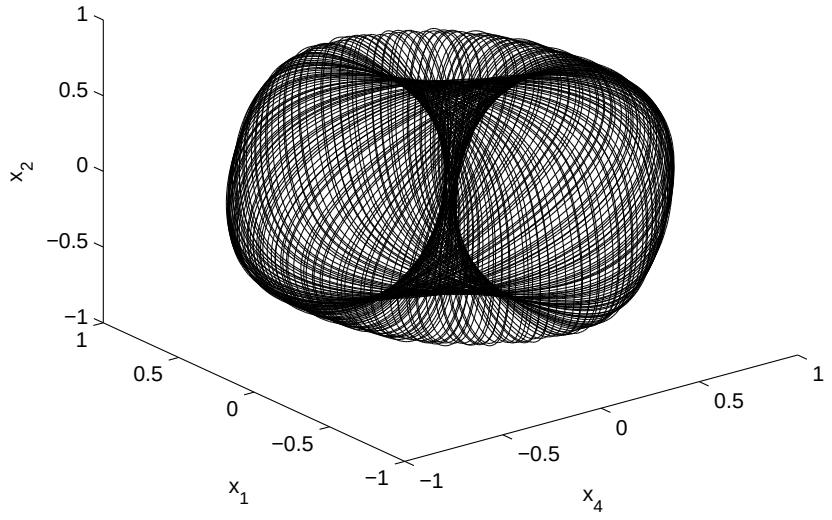

(b)

Figure 3.2: Chaotic attractor of Quantum-CNN system (a)in (x_3, x_4, x_1) space (b)in (x_4, x_1, x_2) space

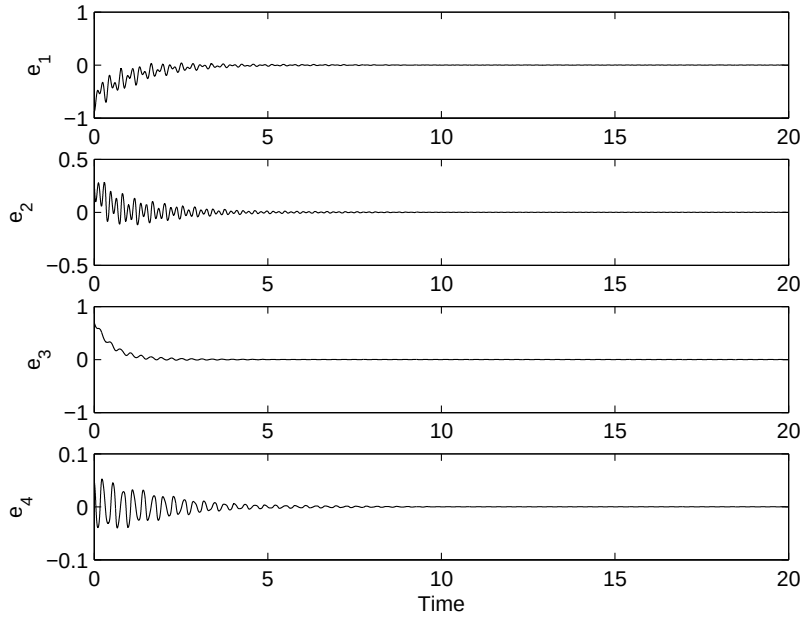

Figure 3.3: Error signals between drive and response system

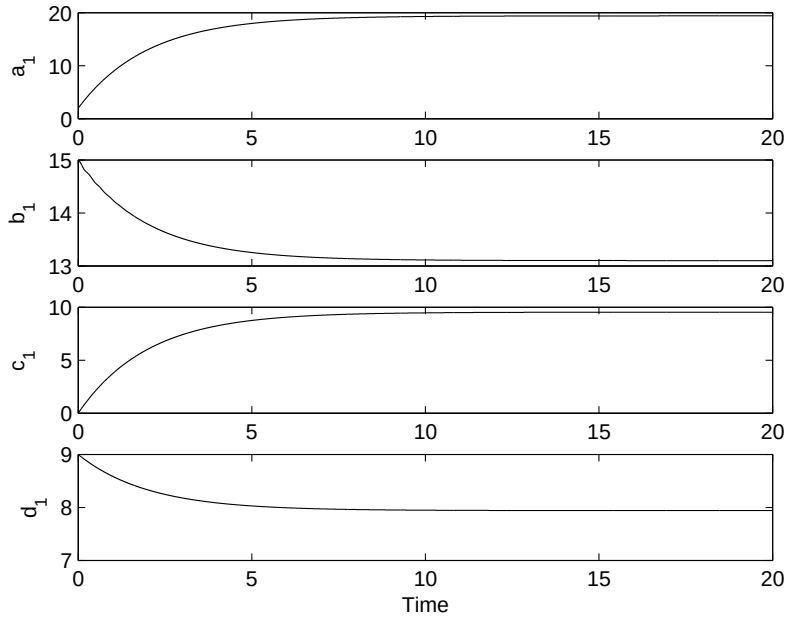

Figure 3.4: Estimated values for unknown parameters

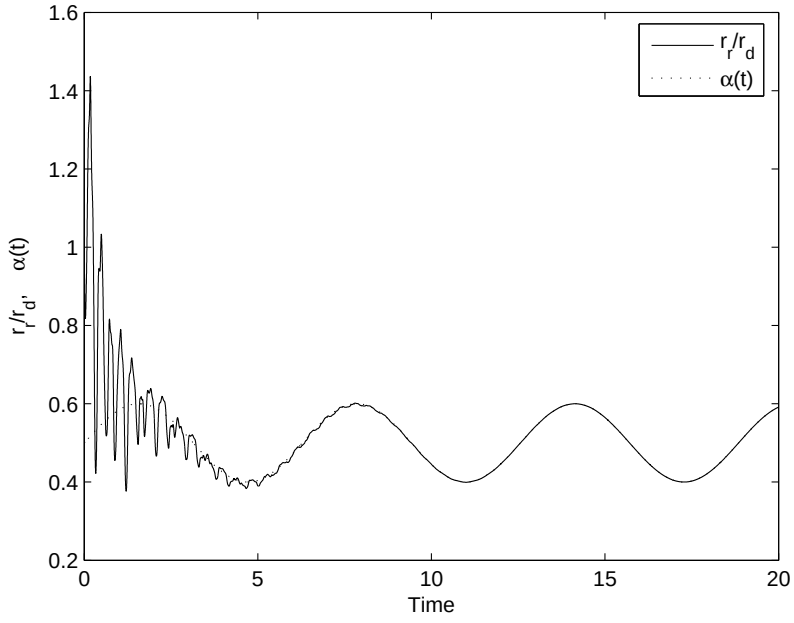

Figure 3.5: Variation of the ratio r_r/r_d and the scaling function $\alpha(t)$

Chapter 4

Modified function projective synchronization between hyperchaotic Lorenz system and Lü system through adaptive nonlinear control

4.1 Introduction

In this chapter we propose a scheme for adaptive modified function projective synchronization(AMFPS) of two hyperchaotic systems. As an application of the proposed AMFPS scheme, synchronization between hyperchaotic Lorenz[120] and hyperchaotic Lü[119] system is studied. Parameters of both drive and response system are assumed to be unknown. Adaptive nonlinear controllers and parameter update rules are derived to obtain MFPS of the systems.

4.2 Modified function projective Synchronization

Consider the following master and slave system

$$\dot{\mathbf{x}} = \mathbf{f}(\mathbf{x}) \tag{4.1}$$

$$\dot{\mathbf{y}} = \mathbf{g}(\mathbf{y}) + \mathbf{u}(\mathbf{x}, \mathbf{y}) \tag{4.2}$$

where $\mathbf{x}, \mathbf{y} \in \mathbf{R}^n$ are the state vectors, $\mathbf{f}, \mathbf{g} : \mathbf{R}^n \to \mathbf{R}^n$ are continuous nonlinear vector functions, $\mathbf{u}(t, \mathbf{x}, \mathbf{y})$ is the vector controller.

We define the error system as

$$\mathbf{e}(t) = \mathbf{y} - \Lambda(t)\mathbf{x} \tag{4.3}$$

where $\Lambda(t)$ is a $n \times n-$ diagonal matrix, i.e $\Lambda(t) = diag(m_1(t), m_2(t), ..., m_n(t))$, and $m_i(t)$ is a continuous differentiable function with $m_i(t) \neq 0$ for all t.

The system (4.1) and (4.2) are said to be in MFPS, if there exists a scaling function matrix $\Lambda(t)$ such that $\lim_{t\to\infty} \|\mathbf{e}(t)\| = 0$.

4.3 Adaptive modified function projective synchronization scheme

Consider a class of uncertain chaotic system described by

$$\dot{x} = f(x) + F(x)\theta, \tag{4.4}$$

where $x \in \mathbf{R}^n$ is the state vector of the system, $\mathbf{f} : \mathbf{R}^n \to \mathbf{R}^n$ is a continuous vector function, $\mathbf{F} : \mathbf{R}^n \to \mathbf{R}^{n\times p}$ is a function matrix, $\theta \in \mathbf{R}^p$ is an unknown parameter vector.

Let system (4.4) be the drive system, then the controlled response system is given by

$$\dot{y} = g(y) + G(y)\phi + u \tag{4.5}$$

where $y \in \mathbf{R}^n$ is the state vector of the system, $\mathbf{g} : \mathbf{R}^n \to \mathbf{R}^n$ is a continuous vector function, $\mathbf{G} : \mathbf{R}^n \to \mathbf{R}^{n\times k}$ is a function matrix,$\phi \in \mathbf{R}^k$ unknown parameter vector of response system, $u \in R^n$ is a controller to be determined. The goal of control is to find out an appropriate u such that the response system is in MFPS with the drive system and the unknown parameters are identified simultaneously.

The error dynamical system between the drive system (4.4) and the response system(4.5) is

$$\begin{aligned} \dot{e} &= \dot{y} - \Lambda(t)\dot{x} - \dot{\Lambda}(t)x \\ &= g(y) + G(y)\phi + u - \Lambda(t)f(x) - \Lambda(t)F(x)\theta - \dot{\Lambda}(t)x \end{aligned} \tag{4.6}$$

Let us choose the controller

$$u = -g(y) - G(y)\hat{\phi} + \Lambda(t)f(x) + \Lambda(t)F(x)\hat{\theta} + \dot{\Lambda}(t)x - ke \tag{4.7}$$

where $\hat{\theta}$ and $\hat{\phi}$ are the estimated values of parameters θ and ϕ and the parameter update rules

$$\begin{aligned} \dot{\hat{\theta}} &= -F(x)^T\Lambda(t)e - l\tilde{\theta} \\ \dot{\hat{\phi}} &= G(y)^T e - h\tilde{\phi} \end{aligned} \tag{4.8}$$

where $\tilde{\theta} = \hat{\theta} - \theta$, $\tilde{\phi} = \hat{\phi} - \phi$ and ,$k = diag(k_1, k_2, ..., k_n)$,$l = diag(l_1, l_2, ..., l_p)$ and $h = diag(h_1, h_2, ..., h_n)$ are positive constant matrices.

From (4.6) and (4.7), the error dynamics is described by

$$\dot{e} = \Lambda(t)F(x)\tilde{\theta} - G(y)\tilde{\phi} - ke \tag{4.9}$$

Hence the MFPS problem becomes the stability of error dynamics (4.9) and update rule (4.8). If it is globally stabilized at the origin, the MFPS of the drive system (4.4) and the response system(4.5) can be globally realized.

Theorem.*For the given scaling function matrix* $\Lambda(t)$*, the MFPS between drive system(4.4) and response system(4.5) will occur by the control law(4.7) and the parameter update rule(4.8)*

Proof: Choose the following Lyapunov function

$$V = \frac{1}{2}[e^T e + \tilde{\theta}^T\tilde{\theta} + \tilde{\phi}^T\tilde{\phi}] \tag{4.10}$$

With the controllers (4.7) and the parameter update rule (4.8), the time derivative of the Lyapunov function along the trajectory of error system (4.6) is

$$\begin{aligned} \dot{V} &= e^T\dot{e} + \tilde{\theta}^T\dot{\tilde{\theta}} + \tilde{\phi}^T\dot{\tilde{\phi}} \\ &= e^T(\Lambda(t)F(x)\tilde{\theta} - G(y)\tilde{\phi} - ke) + \tilde{\theta}^T(-F(x)^T\Lambda(t)e - l\tilde{\theta}) + \tilde{\phi}^T(G(y)^T e - h\tilde{\phi}) \\ &= -e^T ke - \tilde{\theta}^T l\tilde{\theta} - \tilde{\phi}^T h\tilde{\phi} < 0 \end{aligned}$$

Therefore according to the Lyapunov stability theorem, the adaptive MFPS of (4.4) and (4.5) is obtained.

4.4 Adaptive MFPS between hyperchaotic Lorenz system and hyperchaotic Lü system

The hyperchaotic Lorenz system is described as follows[120]:

$$\begin{aligned} \dot{x} &= \alpha(y - x) \\ \dot{y} &= \beta x + y - xz - w \\ \dot{z} &= xy - \gamma z \\ \dot{w} &= \theta yz \end{aligned} \tag{4.11}$$

where x, y, z and w are state variables and $\alpha, \beta, \gamma, \theta$ are parameters. When $\alpha = 10,\ \beta = 28,\ \gamma = 8/3$ and $\theta = 0.1$, the system (4.11) exhibits hyperchaotic behaviour as shown in fig 4.1.

As described in chapter 2, using a feedback controller, a novel hyperchaotic Lü system was constructed based on the original three dimensional Lü system and is given by the following equations[119]:

$$\begin{aligned} \dot{x} &= a(y - x) + w \\ \dot{y} &= -xz + cy \\ \dot{z} &= xy - bz \\ \dot{w} &= xz + dw \end{aligned} \tag{4.12}$$

where x, y, z and w are state variables and a, b, c, d are real constant parameters. When $a = 36,\ b = 3,\ c = 20$ and $-0.35 \leq d \leq 1.3$, the system (4.12) exhibits hyperchaotic behaviour as given in fig.4.2.

In order to achieve the behaviour of MFPS between hyperchaotic Lorenz system and hyperchaotic Lü system, we assume that the hyperchaotic Lorenz system is the drive system whose four variables are denoted by subscript 1 and the hyperchaotic Lü system is the response system whose variables are denoted by subscript 2. The drive and response systems are described, respectively, by the following equations:

$$\begin{aligned} \dot{x}_1 &= \alpha(y_1 - x_1) \\ \dot{y}_1 &= \beta x_1 + y_1 - x_1 z_1 - w_1 \\ \dot{z}_1 &= x_1 y_1 - \gamma z_1 \\ \dot{w}_1 &= \theta y_1 z_1 \end{aligned} \tag{4.13}$$

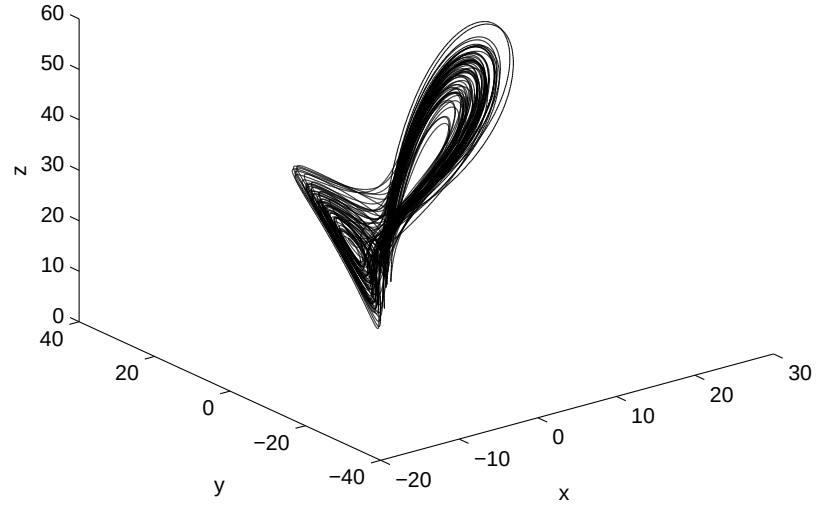

(a)

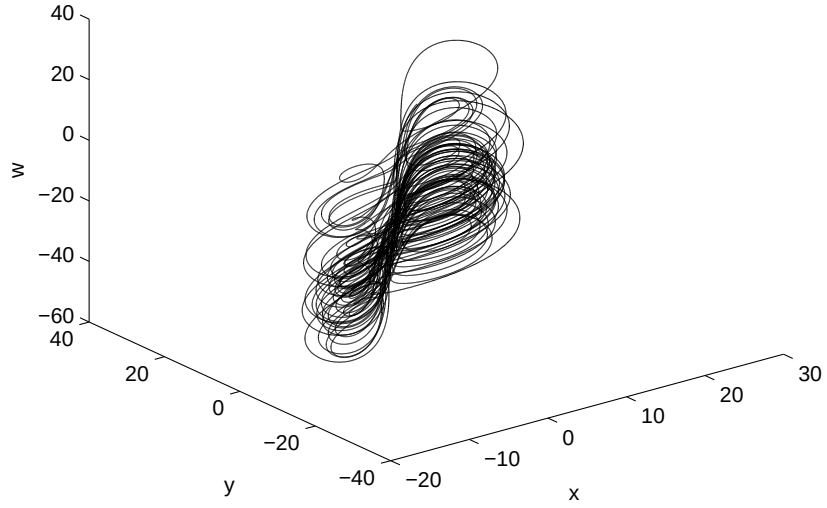

(b)

Figure 4.1: Hyperchaotic attractor of hyperchaotic Lorenz system.(a) in (x, y, z) space (b) in (x, y, w) space.

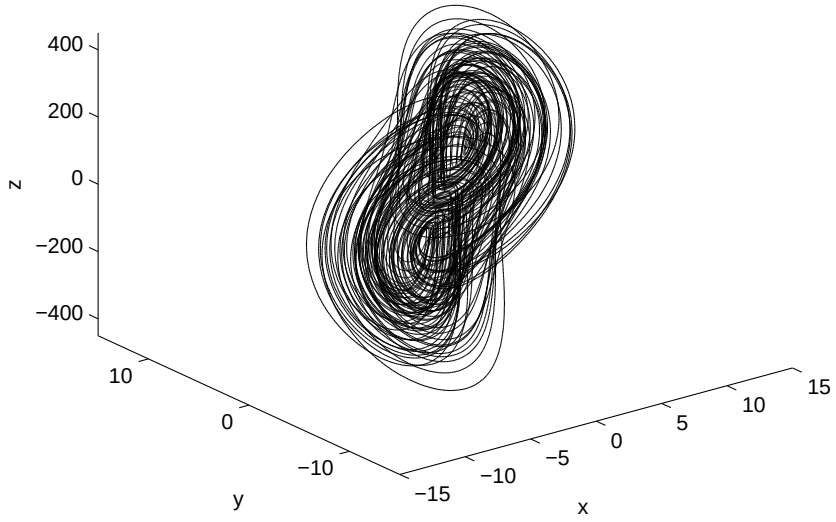

(a)

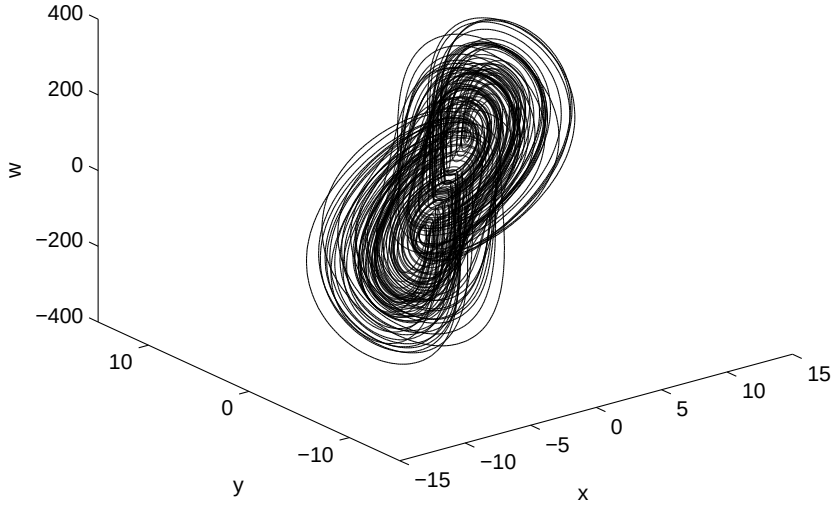

(b)

Figure 4.2: Hyperchaotic attractor of hyperchaotic Lü system (a) in (x, y, z) space (b) in (x, y, w) space.

$$\begin{aligned}
\dot{x}_2 &= a(y_2 - x_2) + w_2 + u_1 \\
\dot{y}_2 &= -x_2 z_2 + c y_2 + u_2 \\
\dot{z}_2 &= x_2 y_2 - b z_2 + u_3 \\
\dot{w}_2 &= x_2 y_2 + d w_2 + u_4
\end{aligned} \tag{4.14}$$

where $U = [u_1, u_2, u_3, u_4]^T$ is the nonlinear controller to be so defined that two chaotic systems can be in MFPS.

Then, according to (4.7) and (4.8) we get the following controller

$$\begin{aligned}
u_1 &= -a_1(y_2 - x_2) - w_2 + m_1(t)\alpha_1(y_1 - x_1) + \dot{m}_1(t)x_1 - k_1 e_1 \\
u_2 &= x_2 y_2 - c_1 y_2 + m_2(t)\beta_1 x_1 + m_2(t) y_1 - m_2(t) x_1 z_1 \\
&\quad - m_2(t) w_1 + \dot{m}_2(t) y_1 - k_2 e_2 \\
u_3 &= -x_2 y_2 + b_1 z_2 + m_3(t) x_1 y_1 - m_3(t)\gamma_1 z_1 + \dot{m}_3(t) z_1 - k_3 e_3 \\
u_4 &= -x_2 z_2 - d_1 w_2 + m_4(t)\theta_1 y_1 z_1 + \dot{m}_4(t) w_1 - k_4 e_4
\end{aligned} \tag{4.15}$$

where $\alpha_1, \beta_1, \gamma_1, \theta_1, a_1, b_1, c_1$ and d_1 are the estimated parameters of the unknown parameters $\alpha, \beta, \gamma, \theta, a, b, c$ and d of the drive and slave systems.

The update rules for the estimated parameters are obtained as

$$\begin{aligned}
\dot{\alpha}_1 &= -m_1(t)(y_1 - x_1)e_1 - h_1(\alpha_1 - \alpha) \\
\dot{\beta}_1 &= -m_2(t) x_1 e_2 - h_2(\beta_1 - \beta) \\
\dot{\gamma}_1 &= m_3(t) z_1 e_3 - h_3(\gamma_1 - \gamma) \\
\dot{\theta}_1 &= -m_4(t) y_1 z_1 e_4 - h_4(\theta_1 - \theta) \\
\dot{a}_1 &= (y_2 - x_2)e_1 - l_1(a_1 - a) \\
\dot{b}_1 &= -z_2 e_3 - l_2(b_1 - b) \\
\dot{c}_1 &= y_2 e_2 - l_3(c_1 - c) \\
\dot{d}_1 &= w_2 e_4 - l_4(d_1 - d)
\end{aligned} \tag{4.16}$$

where $k_i, l_i, h_i > 0 (i = 1, 2, 3, 4)$.

4.5 Numerical simulations

Numerical simulations are presented to demonstrate the effectiveness of the proposed synchronization controller. Fourth-order Runge-Kutta method is used to solve systems(4.13)and(4.14) with time step size 0.001. The parameters are chosen to be $\alpha = 10, \beta = 28, \gamma = 8/3, \theta = 0.1, a = 36,\ b = 3,\ c = 20$ and $d = 1$ in all simulations so that the hyperchaotic Lorenz system and Lü system exhibit chaotic behaviours. The initial conditions of the drive system are $x_1(0) = -1, y_1(0) = -1, z_1(0) = 1$ and $w_1(0) = -1$, and those of the response system are $x_2(0) = 5, y_2(0) = 2, z_2(0) = -5$

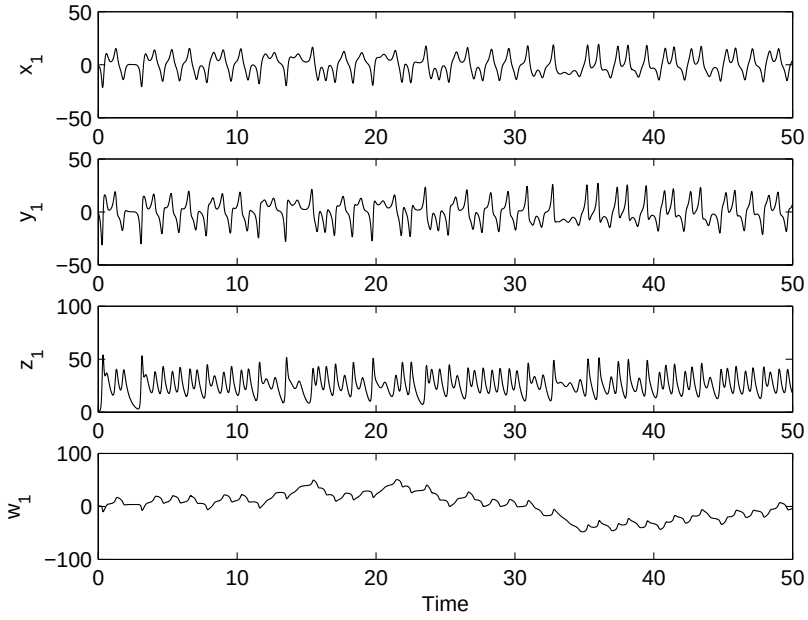

Figure 4.3: The state trajectories of the drive system.

and $w_2(0) = -5$. The initial values of the estimated parameters are chosen as $\alpha_1(0) = 10, \beta_1(0) = 10, \gamma_1(0) = 10, \theta_1(0) = 10, a_1(0) = 10,\ b_1(0) = 10,\ c_1(0) = 10$ and $d_1(0) = 10$. The scaling function matrix elements are chosen as $m_1 = -0.3(5 + 2\sin(2\pi t/10)), m_2 = 1.1(5 + 2\sin(2\pi t/10)), m_3 = -1.7(5 + 2\sin(2\pi t/10))$, and $m_4 = 0.6(5 + 2\sin(2\pi t/10))$.Furthermore, the control gains are chosen as $(k_1, k_2, k_3, k_4) = (1, 1, 1, 1), (l_1, l_2, l_3, l_4) = (1, 1, 1, 1)$ and $(h_1, h_2, h_3, h_4) = (1, 1, 1, 1)$.

The simulation results are shown from Fig.4.3 to Fig. 4.8.The state trajectories of the drive system and the response system when control is not applied and when control applied are depicted in Figs. 4.3, 4.4 and 4.5 respectively. Fig. 4.6 shows the evolution of the MFPS errors, which display the time response of the MFPS errors $e \to 0$ with $t \to \infty$. Figs.4.7 and 4.8 depicts the evolution of the estimated parameters of hyperchaotic Lorenz system and hyperchaotic Lu system, which shows the estimates of the unknown parameters adapt themselves to the true values. These results show that the required synchronization has been achieved with our designed the adaptive control law (4.15) and the parameter update law (4.16).

4.6 Conclusion

This work investigated the MFPS between the hyperchaotic Lorenz system and the Lü system with fully uncertain parameters. On the basis of Lyapunov stability

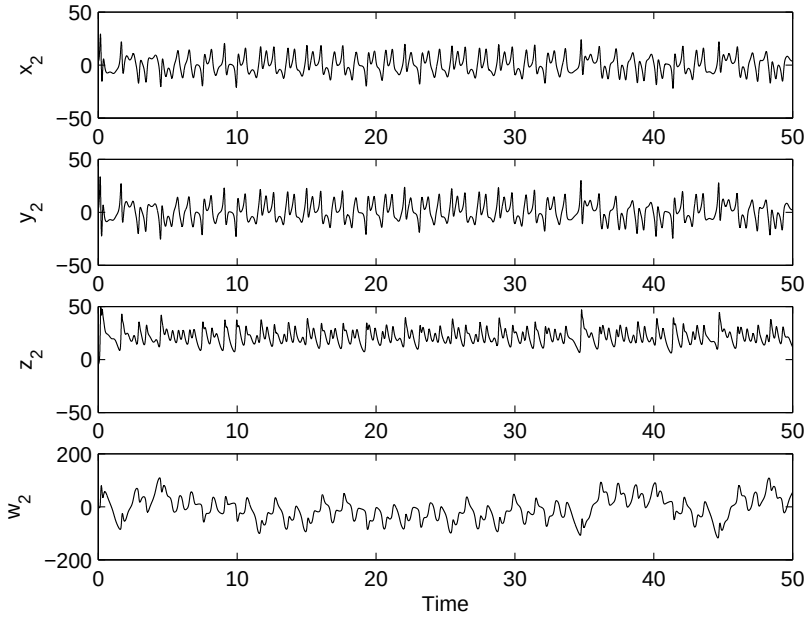

Figure 4.4: The state trajectories of the response system when no control is applied.

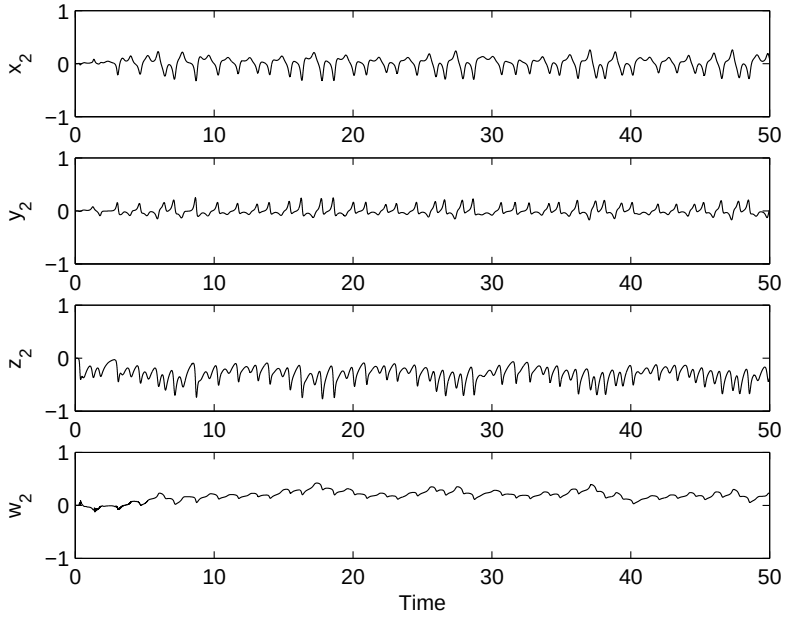

Figure 4.5: The state trajectories of the response system when control is applied.

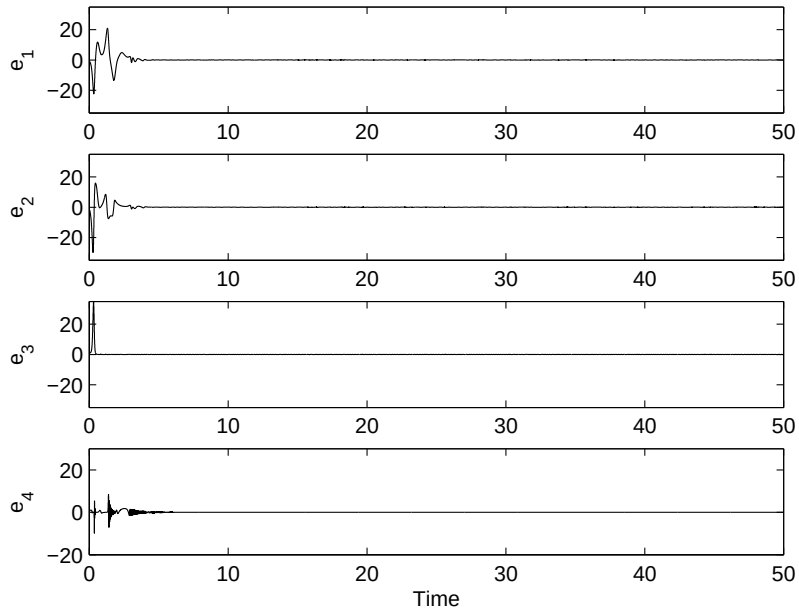

Figure 4.6: The time evolution of MFPS errors between drive and response systems.

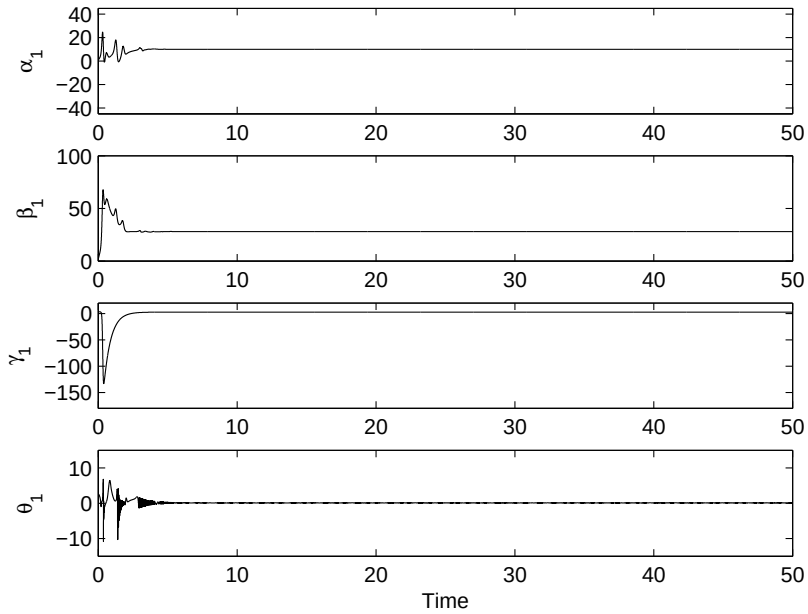

Figure 4.7: The time evolution of the estimated parameters of the hyperchaotic Lorenz system.

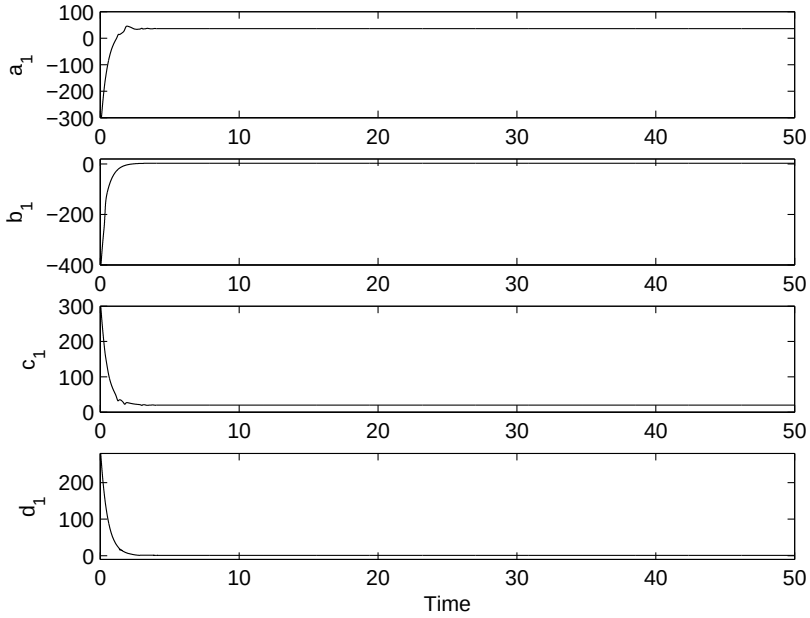

Figure 4.8: The time evolution of the estimated parameters of the hyperchaotic Lü system.

theory, we design adaptive synchronization controllers with corresponding parameter update laws to synchronize the two systems. All the theoretical results are verified by numerical simulations to demonstrate the effectiveness of the proposed synchronization scheme.

Chapter 5

Function projective synchronization in chaotic and hyperchaotic systems through OPCL coupling

5.1 Introduction

Open-plus-closed-loop(OPCL) control method is a more general and physically realizable coupling scheme that can provide stable CS(complete synchronization) and AS(anti-synchronization) in identical and mismatched oscillators. Grosu et. al,[111, 112] recently reported projective synchronization in chaotic systems through open-plus-closed-loop(OPCL) coupling. Hyperchaotic systems possessing at least two positive Lyapunov exponents have more complex behaviour and abundant dynamics than chaotic systems and are more suitable for some engineering applications such as secure communication. Hence how to realize synchronization of hyperchaotic systems through OPCL method is an interesting question.

In this chapter, we propose a physically realizable coupling function through unidirectional OPCL coupling for the FPS of chaotic as well as more complex hyperchaotic systems.

5.2 Unidirectional OPCL coupling for FPS

In chapter 1 we considered the OPCL method for complete synchronization. Here, we briefly discuss the OPCL method for the FPS of two mismatched chaotic or

hyperchaotic oscillators. A chaotic or hyperchaotic driver is defined by

$$\dot{y} = f(y) + \Delta f(y), y \epsilon R^n, \tag{5.1}$$

where $\Delta f(y)$ contains the mismatched terms. It drives another chaotic or hyperchaotic oscillator $\dot{x} = f(x), x \epsilon R^n$ to achieve a goal dynamics $g(t) = \alpha(t)y(t)$,where $\alpha(t)$ is an arbitrary scaling function.

After coupling, the response system is given by

$$\dot{x} = f(x) + D(x, g), \tag{5.2}$$

where the coupling function is defined as

$$D(x, g) = \dot{g} - f(g) + (H - \frac{\partial f(g)}{\partial g})(x - g), \tag{5.3}$$

$\frac{\partial f(g)}{\partial g}$ is the Jacobian of the dynamical system and H is an arbitrary constant Hurwitz matrix $(n \times n)$ whose eigenvalues all have negative real parts.

The error signal of the coupled system is defined by $e = x - g$ and $f(x)$ can be written using Taylor series expansion, as

$$f(x) = f(g) + \frac{\partial f(g)}{\partial g}(x - g) + \cdots . \tag{5.4}$$

Keeping the first-order terms in (5.4) and substituting in (5.2), the error dynamics is obtained as

$$\dot{e} = He \tag{5.5}$$

Since H is a Hurwitz matrix with all of its eigenvalues having negative real parts, $e \longrightarrow 0$ as $t \longrightarrow \infty$ and we obtain asymptotic FPS.

5.3 FPS in chaotic oscillators

5.3.1 Numerical simulation :Identical oscillators

We consider FPS in two identical oscillators using Rössler oscillator systems[116]. The Rössler system arises from work in chemical kinetics and it is given by the

following differential equations.

$$\begin{aligned} \dot{y}_1 &= -\omega y_2 - y_3 \\ \dot{y}_2 &= y_1 + b y_2 \\ \dot{y}_3 &= c + y_3(y_1 - d) \end{aligned} \tag{5.6}$$

which has a chaotic attractor when the system's parameters are chosen as $\omega = 1, b = 0.15, c = 0.2$ and $d = 10$

The Jacobian of the model is

$$\frac{\partial f}{\partial y} = \begin{bmatrix} 0 & -\omega & -1 \\ 1 & b & 0 \\ y_3 & 0 & y_1 - d \end{bmatrix} \tag{5.7}$$

System (5.6) is considered as the drive system. For simplicity, in all simulations the arbitrary Hurwitz matrix is chosen as $-I$.

The response system after coupling is then given by

$$\begin{aligned} \dot{x}_1 &= -\omega x_2 - x_3 + \dot{\alpha} y_1 - e_1 + \omega e_2 + e_3 \\ \dot{x}_2 &= x_1 + b x_2 + \dot{\alpha} y_2 - e_1 - (1 + b) e_2 \\ \dot{x}_3 &= c + x_3(x_1 - d) + \dot{\alpha} y_3 + (\alpha - 1)c + \alpha(1 - \alpha) y_3 y_1 \\ &\quad -\alpha y_3 e_1 - (1 + (\alpha y_1 - d)) e_3 \end{aligned} \tag{5.8}$$

For numerical simulations,the arbitrary scaling function is chosen as $\alpha(t) = 3 + 1.5\sin(2\pi t/10)$. Results of the numerical simulations are shown in figures 5.1 and 5.2. Figure 5.1(a) shows the time series of x_1 and y_1 under OPCL coupling. Figure 5.1(b) depicts the evolution of FPS errors ,which shows errors tending to zero asymptotically. The ratio $\|x\| \,/\, \|y\|$ plotted against time tends to the scaling function as shown in figure 5.2, indicating FPS.

5.3.2 Numerical simulation :Mismatched oscillators

FPS in mismatched case can be illustrated with the example of Lorenz oscillators[6]. The nonlinear differential equations that describe the Lorenz system considered as drive system is given by

$$\begin{aligned} \dot{y}_1 &= \sigma(y_2 - y_1) + \Delta\sigma(y_2 - y_1) \\ \dot{y}_2 &= r y_1 - y_2 - y_1 y_3 + \Delta r y_1 \\ \dot{y}_3 &= -b y_3 + y_1 y_2 - \Delta b y_3 \end{aligned} \tag{5.9}$$

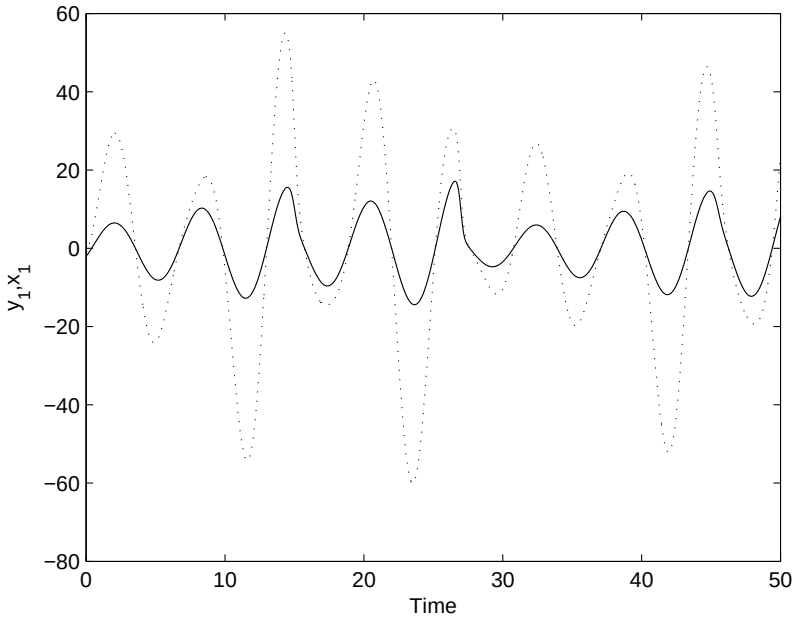

(a)

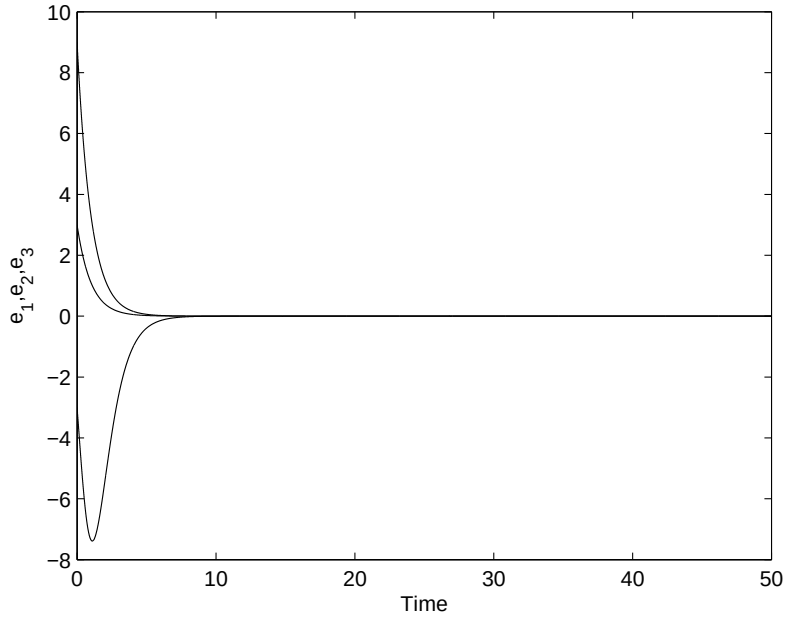

(b)

Figure 5.1: Identical Rössler system. (a)time series of y_1(solid line) and x_1(dashed line)(b)the evolution of FPS errors

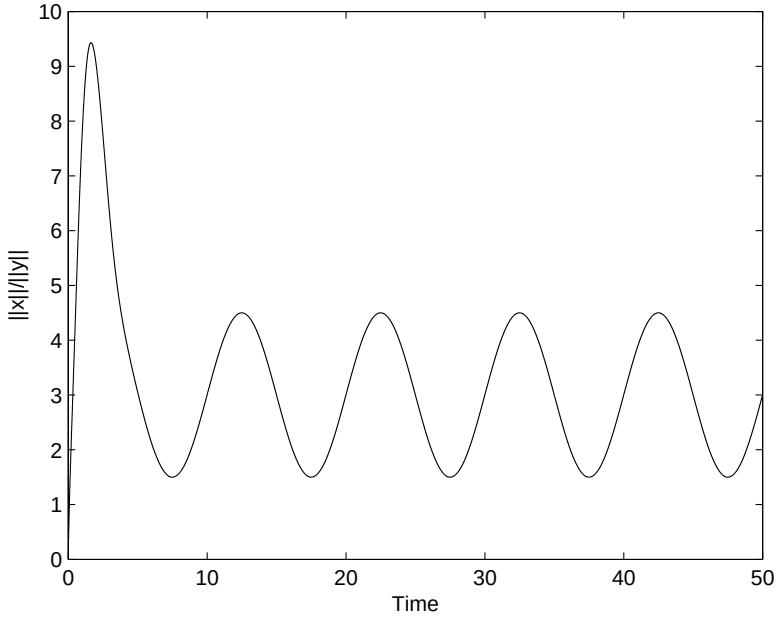

Figure 5.2: Identical Rössler system. $\|x\| / \|y\|$ plotted against time tends to the scaling function

which has a chaotic attractor when the parameters are respectively chosen as $\sigma = 10, b = \frac{8}{3}, r = 28$.

The Jacobian of the system is

$$\frac{\partial f}{\partial y} = \begin{bmatrix} -\sigma & \sigma & 0 \\ (r - y_3) & -1 & -y_1 \\ y_2 & y_1 & -b \end{bmatrix} \tag{5.10}$$

The response system after the OPCL coupling is given by

$$\begin{aligned} \dot{x}_1 &= \sigma(x_2 - x_1) + \alpha\Delta\sigma(y_2 - y_1) \\ &\quad +\dot{\alpha}y_1 - (1 - \sigma)e_1 - \sigma e_2 \\ \dot{x}_2 &= rx_1 - x_2 - x_1x_3 + \alpha(\alpha - 1)y_1y_3 \\ &\quad +\alpha\Delta ry_1 + \dot{\alpha}y_2 - (r - \alpha y_3)e_1 + \alpha y_1e_3 \\ \dot{x}_3 &= -bx_3 + x_1x_2 + \alpha(1 - \alpha)y_1y_2 - \alpha\Delta by_3 \\ &\quad +\dot{\alpha}y_3 - \alpha y_2e_1 - \alpha y_1e_2 - (1 - b)e_3 \end{aligned} \tag{5.11}$$

For numerical simulations,the driver is chosen identical to the response except

that $\Delta r = 5$ and the arbitrary scaling function is chosen as $\alpha(t) = 5 + 2\cos(2\pi t/15)$. Results of the numerical simulations are shown in figures 5.3-5.4.

5.4 FPS in Hyperchaotic oscillators

5.4.1 Numerical simulation :Identical oscillators

Hyperchaotic systems possessing more than one positive Lyapunov exponents exhibit rich and complex dynamics than chaotic systems and are more suitable for some applications like secure communications. In this section we apply OPCL control to obtain FPS in two identical hyperchaotic Lorenz systems. The hyperchaotic Lorenz system[120] is described by following nonlinear differential equations

$$\begin{aligned} \dot{y}_1 &= a(y_2 - y_1) \\ \dot{y}_2 &= \beta y_1 + y_2 - y_1 y_3 - y_4 \\ \dot{y}_3 &= y_1 y_2 - \gamma y_3 \\ \dot{y}_4 &= \theta y_2 y_3 \end{aligned} \tag{5.12}$$

The system exhibits hyperchaotic behaviour when $a = 10, \beta = 28, \gamma = 8/3$ and $\theta = 0.1$.

The Jacobian is given by

$$\frac{\partial f}{\partial y} = \begin{bmatrix} -a & a & 0 & 0 \\ (\beta - y_3) & 1 & -y_1 & -1 \\ y_2 & y_1 & -\gamma & 0 \\ 0 & \theta y_3 & \theta y_2 & 0 \end{bmatrix} \tag{5.13}$$

An identical response system after coupling is then given by

$$\begin{aligned} \dot{x}_1 &= a(x_2 - x_1) + \dot{\alpha} y_1 - (1-a)e_1 - a e_2 \\ \dot{x}_2 &= \beta x_1 + x_2 - x_1 x_3 - x_4 + \alpha(\alpha - 1) y_1 y_3 \\ &\quad + \dot{\alpha} y_2 - (\beta - \alpha y_3)e_1 - 2e_2 + \alpha y_1 e_3 + e_4 \\ \dot{x}_3 &= x_1 x_2 - \gamma x_3 + \alpha(1-\alpha) y_1 y_2 \\ &\quad + \dot{\alpha} y_3 - \alpha y_2 e_1 - \alpha y_1 e_2 - (1-r)e_3 \\ \dot{x}_4 &= \theta x_2 x_3 + \alpha(1-\alpha)\theta y_2 y_3 \\ &\quad + \dot{\alpha} y_4 - \theta\alpha y_3 e_2 - \theta\alpha y_3 e_3 - e_4 \end{aligned} \tag{5.14}$$

Simulation results when the arbitrary scaling function matrix is chosen as $\alpha(t) =$

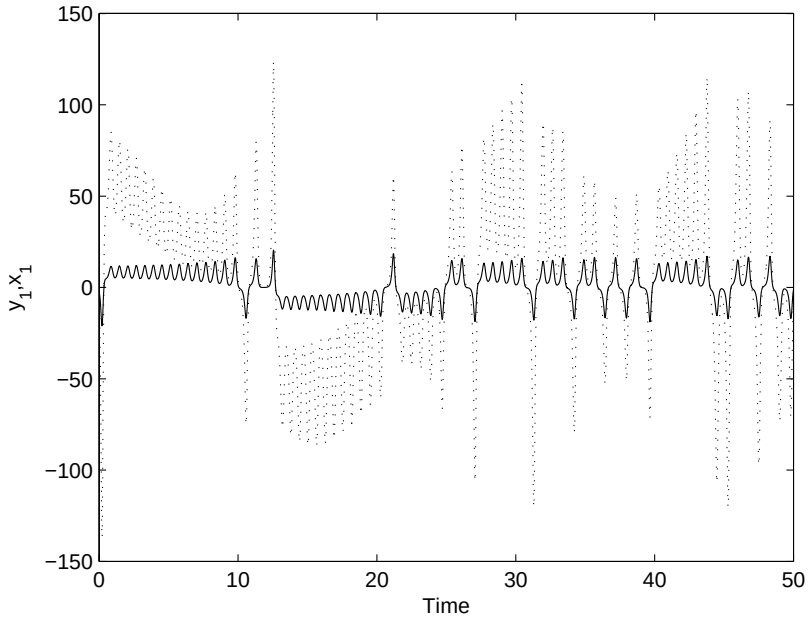

(a)

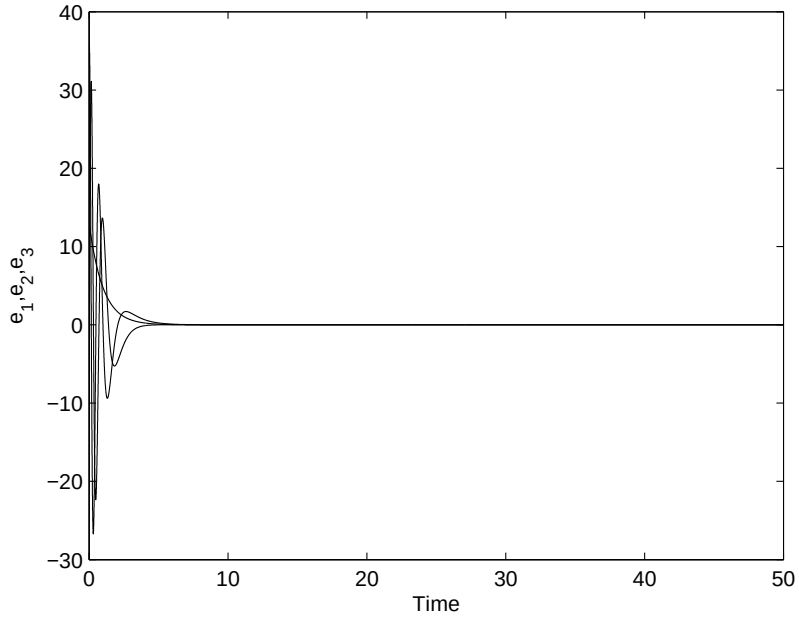

(b)

Figure 5.3: Mismatched Lorenz system. Driver identical to response exceptΔr = 5(a)time series of y_1(solid line) and x_1(dashed line)(b)the evolution of FPS errors

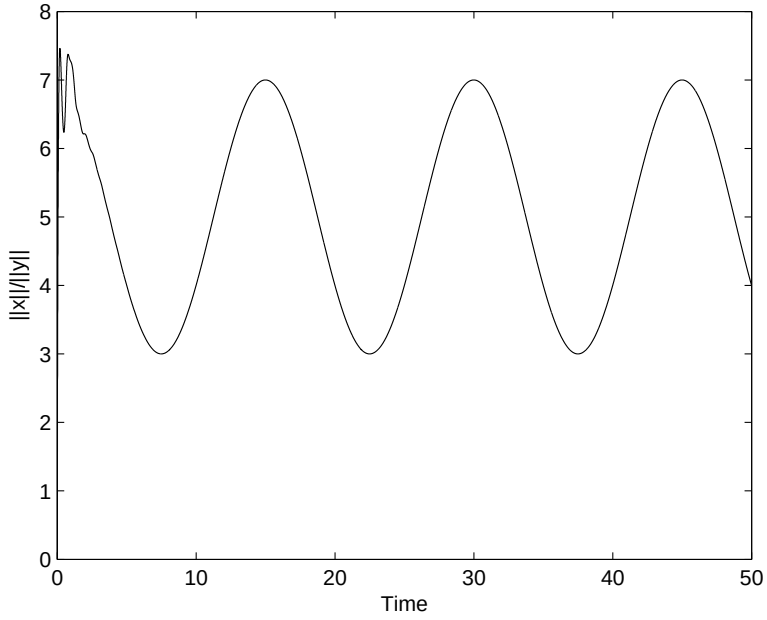

Figure 5.4: Mismatched Lorenz system. $\|x\| \,/\, \|y\|$ plotted against time tends to the scaling function

$5 + 2\cos(2\pi t/15 + 10)$ is depicted in figures 5.5-5.6.

5.4.2 Numerical simulation :Mismatched oscillators

For the mismatched case we choose hyperchaotic Chen [121]oscillators. The hyperchaotic Chen system with mismatch which is chosen as driver is given by

$$\begin{aligned} \dot{y}_1 &= a(y_2 - y_1) + y_4 + \Delta a(y_2 - y_1) \\ \dot{y}_2 &= dy_1 - y_1 y_3 + cy_2 + \Delta dy_1 + \Delta cy_2 \\ \dot{y}_3 &= y_1 y_2 - by_3 - \Delta by_3 \\ \dot{y}_4 &= y_2 y_3 + ry_4 + \Delta ry_4 \end{aligned} \tag{5.15}$$

When $a = 35, b = 3, c = 12, d = 7, 0.085 \leq r \geq 0.798$, system is hyperchaotic. The Jacobian is

$$\frac{\partial f}{\partial y} = \begin{bmatrix} -a & a & 0 & 1 \\ (d - y_3) & c & -y_1 & 0 \\ y_2 & y_1 & -b & 0 \\ 0 & y_3 & y_2 & r \end{bmatrix} \tag{5.16}$$

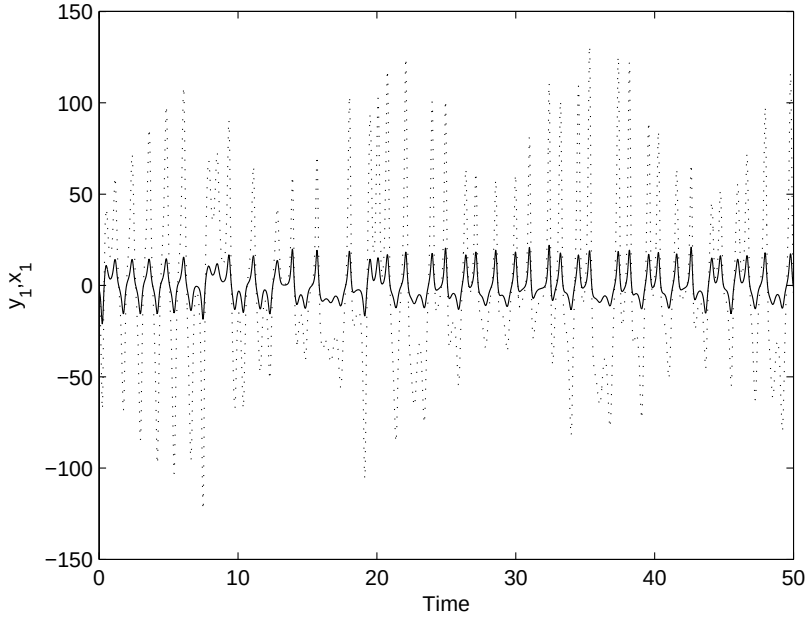

(a)

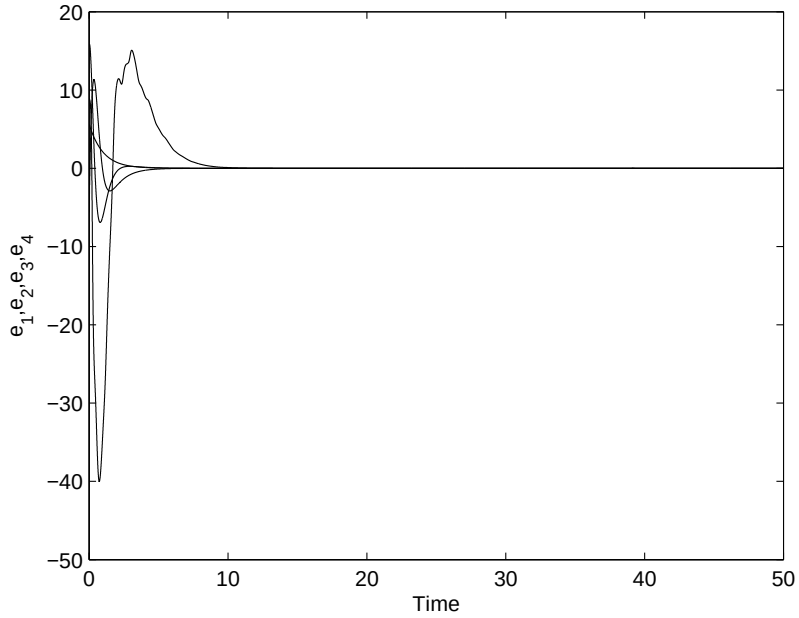

(b)

Figure 5.5: Identical hyperchaotic Lorenz system. (a)time series of y_1(solid line) and x_1(dashed line)(b)the evolution of FPS errors

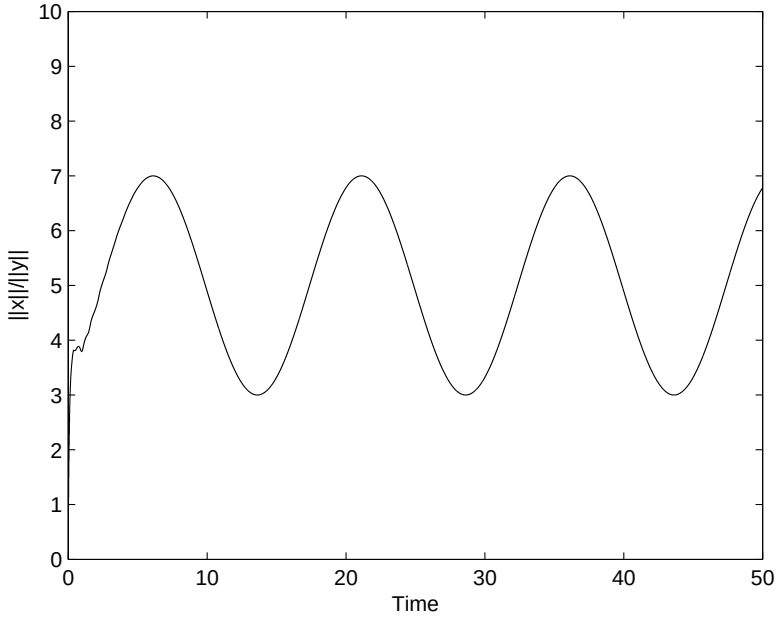

Figure 5.6: Identical hyperchaotic Lorenz system. $\|x\| / \|y\|$ plotted against time tends to the scaling function

The response system after coupling is obtained as

$$\begin{aligned}
\dot{x}_1 &= a(x_2 - x_1) + x_4 + \dot{\alpha} y_1 \\
&\quad -(1-a)e_1 - ae_2 - e_4 \\
\dot{x}_2 &= dx_1 - x_1 x_3 + cx_2 + \alpha(\alpha - 1) y_1 y_3 + \dot{\alpha} y_2 + \alpha \Delta d y_1 \\
&\quad +\alpha \Delta c y_2 - (d - \alpha y_3)e_1 - (1+c)e_2 + \alpha y_1 e_3 \\
\dot{x}_3 &= x_1 x_2 - bx_3 + \alpha(1-\alpha) y_1 y_2 + \dot{\alpha} y_3 \\
&\quad -\alpha y_2 e_1 - \alpha y_1 e_2 - (1-b)e_3 \\
\dot{x}_4 &= x_2 x_3 + rx_4 + \alpha(1-\alpha) y_2 y_3 + \alpha \Delta r y_4 \\
&\quad +\dot{\alpha} y_4 - \alpha y_3 e_2 - \alpha y_2 e_3 - (1+r)e_4
\end{aligned} \tag{5.17}$$

For numerical simulations,the parameters of the system are selected as $a = 35, b = 3, c = 12, d = 7$ and $r = 0.2$. The mismatch in parameters are chosen as $\Delta a = 0, \Delta b = 0, \Delta c = 0, \Delta d = 0$ and $\Delta r = 0.5$ so that both the drive and response Chen systems exhibits hyperchaotic behaviour. The arbitrary scaling function is chosen as $\alpha(t) = 4 + 2\sin(2\pi t/10 + 20)$. The simulation results indicated in Fig 5.7-5.8 show that the two mismatched systems are in FPS.

5.5 Conclusions

FPS is a more general definition of synchronization. In FPS, the master and slave system synchronize upto a scaling function which can be used get more secure communication in application to secure communication because it is obvious that the unpredictability of the scaling function can additionally enhance the security of communication.The OPCL coupling method is a physically realizable method which is suited for practical applications.We design controls through OPCL coupling for the FPS of identical as well as mismatched chaotic and hyperchaotic systems.Numerical simulations verify robust FPS.

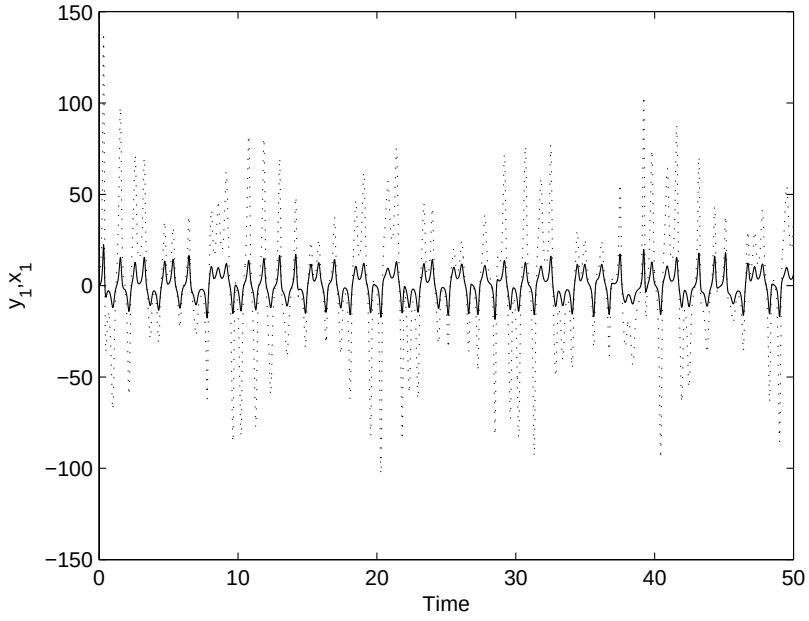

(a)

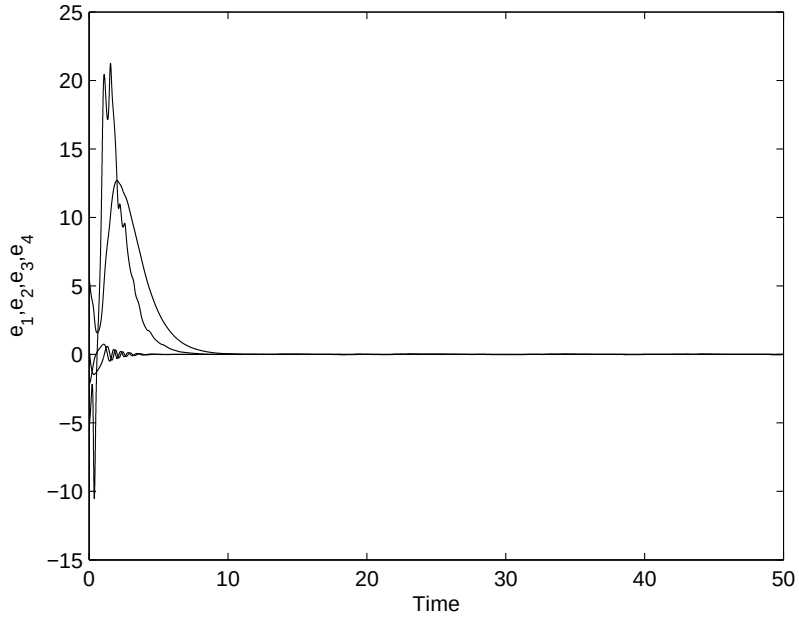

(b)

Figure 5.7: Mismatched hyperchaotic Chen system. Driver identical to response except$\Delta r = 0.5$ (a)time series of y_1(solid line) and x_1(dashed line)(b)the evolution of FPS errors

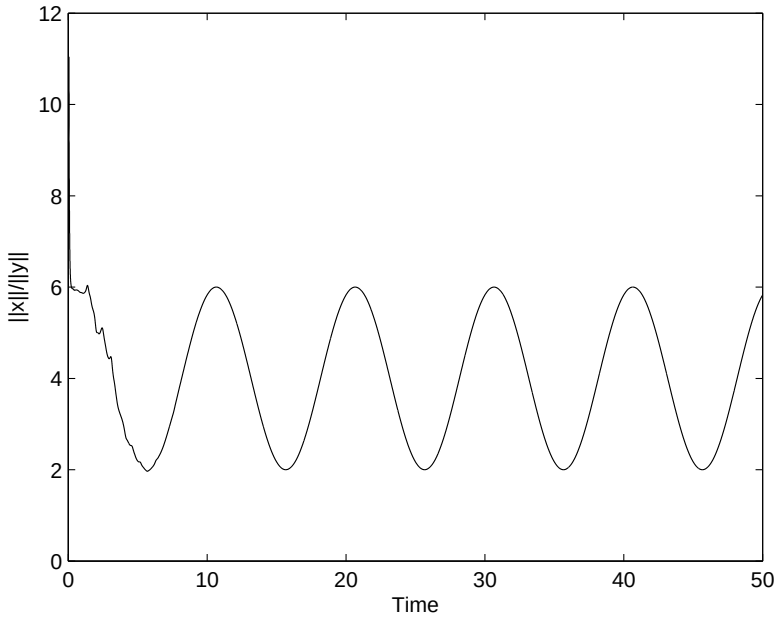

Figure 5.8: Mismatched hyperchaotic Chen system. $\|x\| \,/\, \|y\|$ plotted against time tends to the scaling function

Chapter 6

Modified function projective synchronization in hyperchaotic systems through OPCL coupling

6.1 Introduction

In this chapter, we propose a scheme for realizing the MFPS of hyperchaotic systems through OPCL coupling. We design controllers to obtain MFPS of two identical hyperchaotic Rössler systems[122] and mismatched hyperchaotic Lü systems[119]. A secure communication scheme based on MFPS is also investigated.

6.2 MFPS through OPCL coupling

MFPS is an extension of FPS where drive and response systems are synchronized upto a desired scaling function matrix $m(t) = diag[m_1(t), m_2(t), ..., m_n(t)]^T$. The new goal dynamics $\tilde{g}(t)$ is given by $\tilde{g}(t) = [g_1(t), g_2(t), g_3(t), g_4(t)]^T = [m_1(t)y_1(t), m_2(t)y_2(t), m_3(t)y_3(t), m_4(t)y_4(t)]^T$ for the four dimensional case.

The response system after coupling becomes

$$\dot{x} = f(x) + D(x, \tilde{g}), \tag{6.1}$$

where the coupling function is defined by

$$\begin{aligned} D(x,\widetilde{g}) &= \begin{bmatrix} m_1(t)\dot{y}_1(t) \\ m_2(t)\dot{y}_2(t) \\ m_3(t)\dot{y}_3(t) \\ m_4(t)\dot{y}_4(t) \end{bmatrix} + \begin{bmatrix} \dot{m}_1(t)y_1(t) \\ \dot{m}_2(t)y_2(t) \\ \dot{m}_3(t)y_3(t) \\ \dot{m}_4(t)y_4(t) \end{bmatrix} - f(\tilde{g}) \\ &+(H - \frac{\partial f(\tilde{g})}{\partial \tilde{g}}) \begin{bmatrix} x_1(t) - m_1(t)y_1(t) \\ x_2(t) - m_2(t)y_2(t) \\ x_3(t) - m_3(t)y_3(t) \\ x_4(t) - m_4(t)y_4(t) \end{bmatrix} \end{aligned} \tag{6.2}$$

Now as in chapter 4, we define the errors $e = (e_1, e_2, e_3, e_4)^T = (x_1(t) - m_1(t)y_1(t), x_2(t) - m_2(t)y_2(t), x_3(t) - m_3(t)y_3(t), x_4(t) - m_4(t)y_4(t))^T$. If $e \longrightarrow 0$ asymptotically we obtain MFPS.

6.3 MFPS of two identical Rössler hyperchaotic systems

Hyperchaotic Rössler system [122]is described by the following nonlinear differential equations

$$\begin{aligned} \dot{y}_1 &= -y_2 - y_3 \\ \dot{y}_2 &= y_1 + ay_2 + y_4 \\ \dot{y}_3 &= b + y_1 y_3 \\ \dot{y}_4 &= -cy_3 + dy_4 \end{aligned} \tag{6.3}$$

The system exhibits hyperchaotic behaviour when $a = 0.25, b = 3, c = 0.5$ and $d = 0.05$.

The response system after coupling ,choosing the arbitrary Hurwitz matrix $H =$

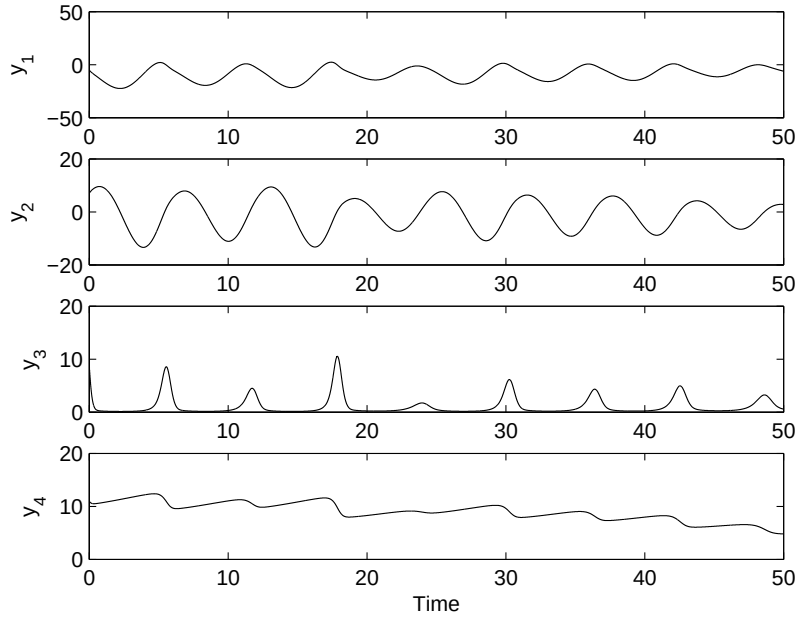

Figure 6.1: Time evolution of the drive system(6.3) states.

$-I_4$ is given by

$$\begin{aligned}
\dot{x}_1 &= -x_2 - x_3 + (m_2 - m_1)y_2 + (m_3 - m_1)y_3 + \dot{m}_1 y_1 \qquad (6.4)\\
&\quad -e_1 + e_2 + e_3\\
\dot{x}_2 &= x_1 + ax_2 + x_4 + (m_2 - m_1)y_1 + (m_2 - m_4)y_4 + \dot{m}_2 y_2\\
&\quad +e_1 - (a+1)e_2 - e_4\\
\dot{x}_3 &= b + x_1 x_3 + (m_3 - 1)b + (1 - m_1)m_3 y_1 y_3 + \dot{m}_3 y_3\\
&\quad -m_3 y_3 e_1 - (1 + m_1 y_1)e_2\\
\dot{x}_4 &= -cx_3 + dx_4 + (m_3 - m_4)cy_3 + \dot{m}_4 y_4\\
&\quad +ce_3 - (1+d)e_4 \qquad (6.5)
\end{aligned}$$

For numerical simulations, we choose the arbitrary scaling function matrix elements as $m_1(t) = 0.05 + 0.03sin(t), m_2(t) = 0.04 + 0.02cos(2\pi t), m_3(t) = 0.03 + 0.015sin(2\pi t/20{+}50)$ and $m_4(t) = 0$. The results of numerical simulations are shown in figures (6.1)-(6.3). Figure 6.1 shows the time evolution of the state variables of the drive and figure 6.2 that of the response system under coupling. Fig 6.3 displays the evolution of errors tending to zero asymptotically indicating MFPS.

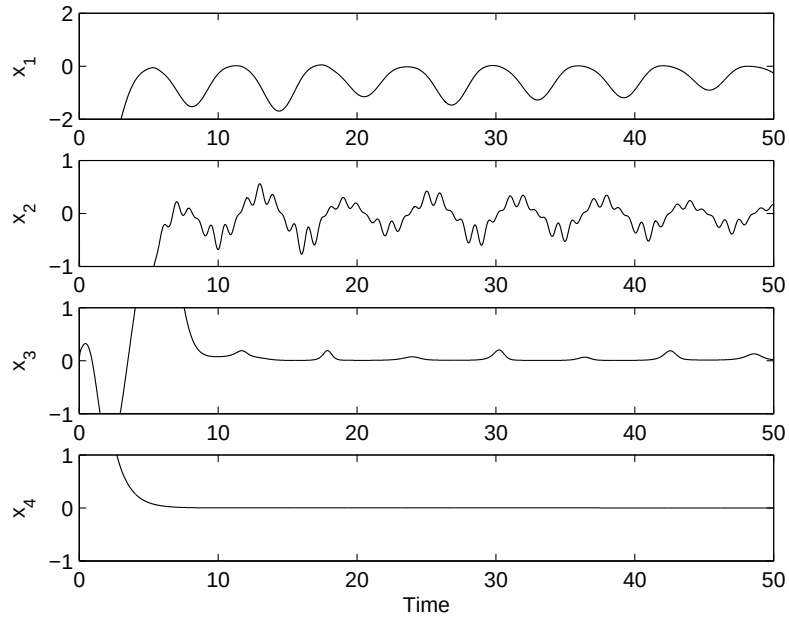

Figure 6.2: Time evolution of the response system(6.4) states.

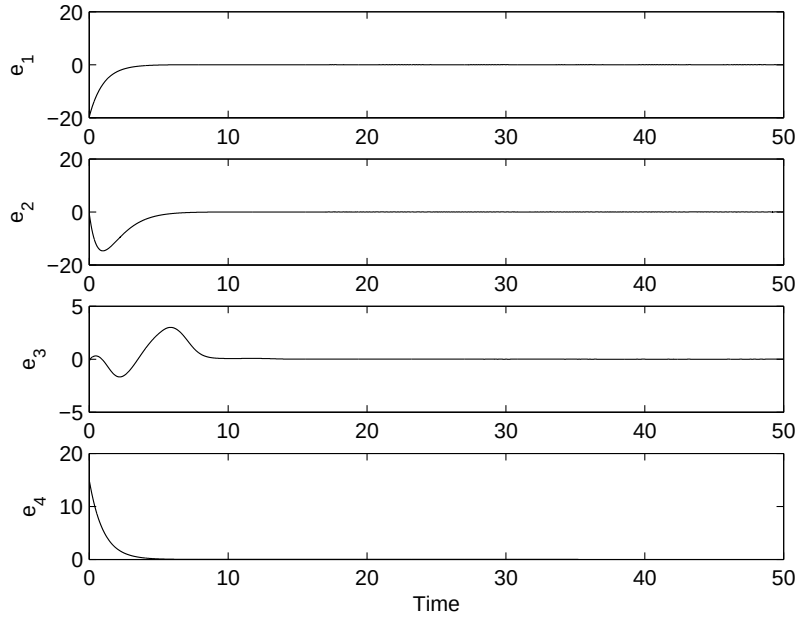

Figure 6.3: The time evolution of MFPS errors between drive(6.3) and response system(6.4).

6.4 MFPS of two mismatched Lü hyperchaotic systems

To study MFPS in mismatched oscillators,we choose Lü hyperchaotic system[119]. The Lü hyperchaotic system with mismatch considered as the driver is given by

$$\begin{aligned} \dot{y}_1 &= a(y_2 - y_1) + y_4 \\ \dot{y}_2 &= -y_1 y_3 + c y_2 \\ \dot{y}_3 &= y_1 y_2 - b y_3 \\ \dot{y}_4 &= y_1 y_3 + d y_4 + \Delta d y_4 \end{aligned} \tag{6.6}$$

where Δd is the parameter mismatch. The system exhibits hyperchaotic behaviour when $a = 36, b = 3, c = 20$ and $-0.35 < d \leq 1.30$.

The response system after coupling is obtained as

$$\begin{aligned} \dot{x}_1 &= a(x_2 - x_1) + x_4 + (m_1 - m_2)a y_2 + (m_1 - m_4)y_4 + \dot{m}_1 y_1 \\ &\quad -(1-a)e_1 - a e_2 - e_4 \\ \dot{x}_2 &= -x_1 x_3 + c x_2 + (m_1 m_3 - m_2) y_1 y_3 + \dot{m}_2 y_2 \\ &\quad + m_3 y_3 e_1 - (1+c)e_2 + m_1 y_1 e_3 \\ \dot{x}_3 &= x_1 x_2 - b x_3 + (m_3 - m_1 m_2) y_1 y_2 + \dot{m}_3 y_3 \\ &\quad - m_2 y_2 e_1 - m_1 y_1 e_2 + (b-1)e_3 \\ \dot{x}_4 &= x_1 x_3 + d x_4 + (m_4 - m_1 m_3) y_1 y_3 + m_4 \Delta d y_4 + \dot{m}_4 y_4 \\ &\quad - m_3 y_3 e_1 - m_1 y_1 e_3 - (1+d)e_4 \end{aligned} \tag{6.7}$$

Numerical simulations are performed by choosing the arbitrary scaling function matrix elements as $m_1(t) = 0.03 + 0.02sin(2\pi t/10 + 20), m_2(t) = 0.02 + 0.01cos(2\pi t/10), m_3(t) = 0.05 + 0.025sin(2\pi t/20)$ and $m_4(t) = 0.03 + 0.015sin(2\pi t/10 + 15)$. The parameters of the drive and response systems are selected as $a = 36, b = 3, c = 20$ and $d = 1$ and the parameter mismatch Δd is chosen as -0.5.Figure 6.4 and 6.5 display respectively, time response of the states of the drive and response systems under OPCL coupling for MFPS. The synchronization errors asymptotically tending to zero is depicted in figure 6.6.

6.5 Application of MFPS in secure communication

MFPS with the unpredictability of the scaling function matrix can provide enhanced security in secure communication. In this section, a scheme for secure communication based on MFPS is investigated in theory. Fig. 6.7 shows a block diagram of the

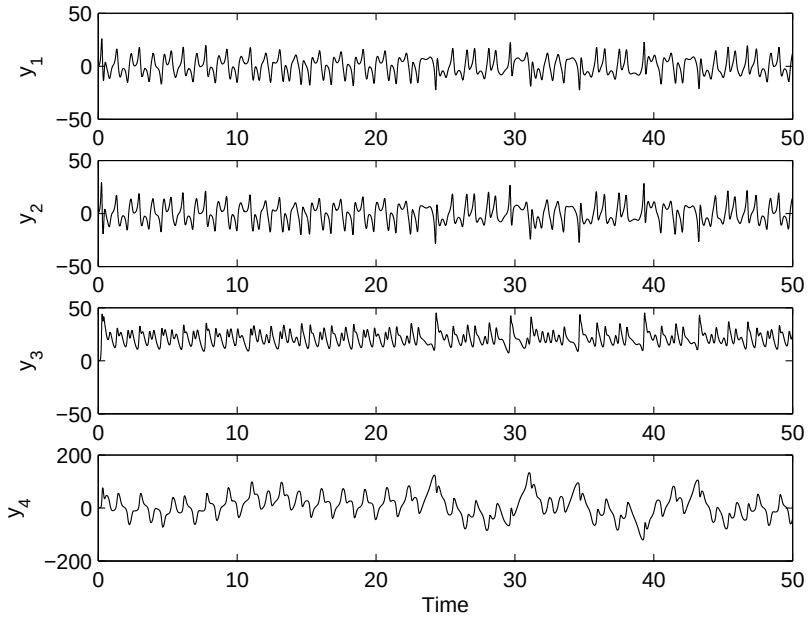

Figure 6.4: Time evolution of the drive system(6.6) states.

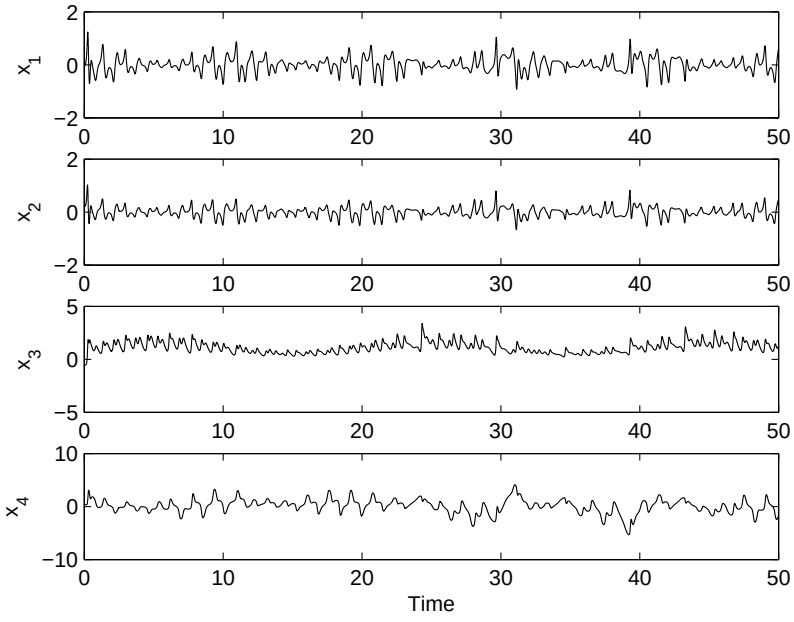

Figure 6.5: Time evolution of the response system(6.7) states.

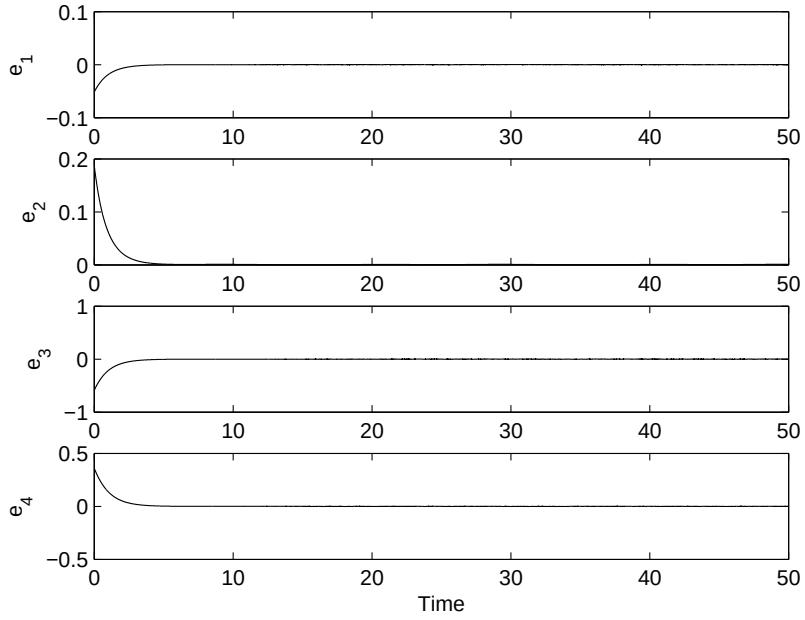

Figure 6.6: The time evolution of MFPS errors between drive(6.6) and response system(6.7).

communication scheme in which L1 and L2 are hyperchaotic Lü systems which are used as the transmitter and receiver, respectively. $m_s(t)$ is the information signal that has to be send through the communication channel securely. The information signal is added to the dynamics of the chaotic system by changing $y_2 \rightarrow y_2 + m_s(t)$. Thus the chaotic driver is obtained as

$$\begin{aligned} \dot{y}_1 &= a((y_2 + m_s(t)) - y_1) + y_4 \\ \dot{y}_2 &= -y_1 y_3 + c(y_2 + m_s(t)) \\ \dot{y}_3 &= y_1(y_2 + m_s(t)) - by_3 \\ \dot{y}_4 &= y_1 y_3 + dy_4 + \Delta dy_4 \end{aligned} \tag{6.8}$$

Under the application of the control signal D to the receiver, MFPS of driver and receiver is achieved and the information signal recovered at the receiving end $m_r(t)$ is obtained as $m_r(t) = (x_2 - m_2(t)y_2)/m_2(t)$. The time evolution of the information signal $m_s(t)$ and the recovered signal $m_r(t)$ displayed in fig.6.8 show that the information signal $m_s(t)$ is recovered after a short transient.

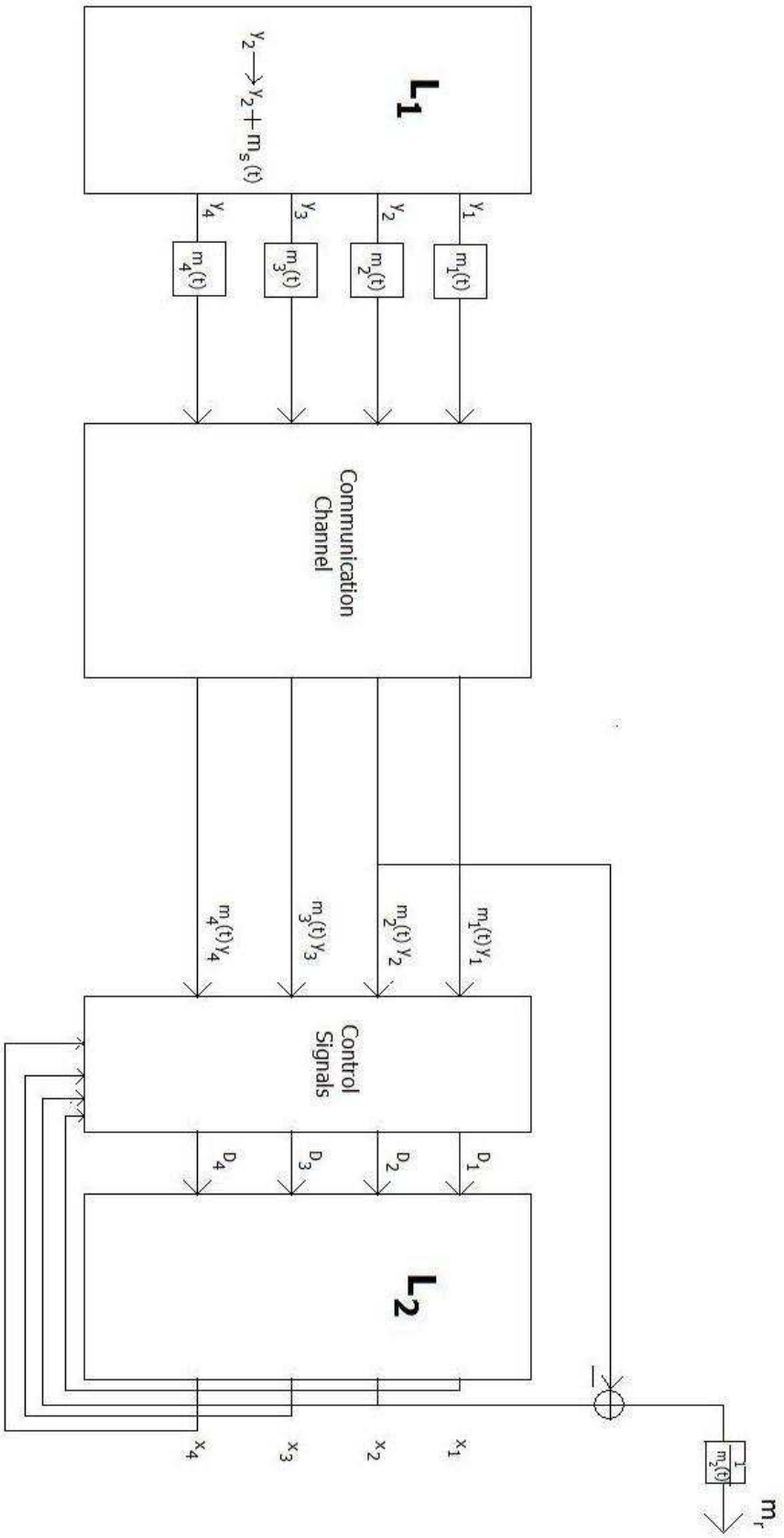

Figure 6.7: Communication scheme based on MFPS.

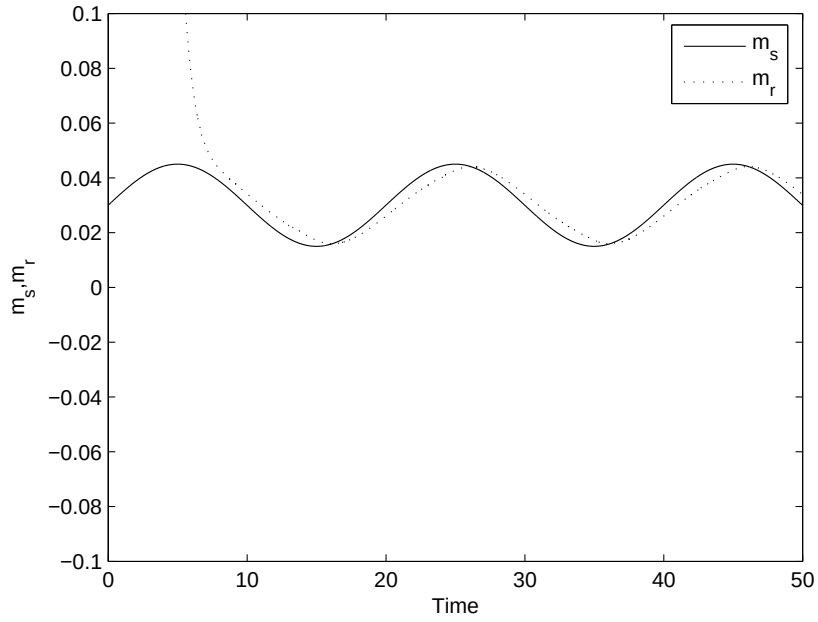

Figure 6.8: The time evolution of information signal $m_s(t)$ and the recovered signal $m_r(t)$

6.6 Conclusion

This work investigated the MFPS of two identical and mismatched hyperchaotic systems. Based on unidirectional OPCL coupling, we design controllers to realize MFPS of two hyperchaotic systems. A scheme for secure communication based on MFPS is also presented. All the theoretical results are verified by numerical simulations to demonstrate the effectiveness of the proposed synchronization schemes.

Chapter 7

Summary

FPS is a more general form of synchronization. Hyperchaotic systems possessing more than one positive Lypaunov exponent exhibit highly complex behaviour and are more suitable for some applications like secure communications. In this thesis we report studies of FPS and MFPS of a few chaotic and hyperchaotic systems. When all the parameters of the system are known we show that active nonlinear control method can be effectively used to obtain FPS. Adaptive nonlinear control and OPCL control method are employed for obtaining FPS and MFPS when some or all parameters of the system are uncertain. A secure communication scheme based on MFPS is also proposed in theory. All our theoretical calculations are verified by numerical simulations.

Bibliography

[1] J. H. Poincaré , Acta Mathematica **13**, 1 (1890).

[2] B.Van der Pol and J. Van der Mark, Nature **120**,363(1927)

[3] M. L. Cartwright and J. E. Littlewood, Journal of the London Mathematical Society **20**,180(1945)

[4] N. Levinson, Ann. Math. **50,**127(1949)

[5] S. Smale, Bull. Amer. Math. Soc.**73**, 747(1967).

[6] E. Lorenz, J. Atmos. Sci. **20**,130 (1963)

[7] Y. Ueda, C. Hayashi, N. Akamatsu, and H. Itakura, Electronics & Communication in Japan **53**,31(1970)

[8] T.Y. Li and J.A. Yorke, Amer. Math. Monthly **82**,985(1975)

[9] R.M. May, Nature **261**,459(1976).

[10] J. P. Gollub and H. L. Swinney, Phys. Rev Lett. **35**, 927 (1975).

[11] M. Lakshmanan and S. Rajasekar,*Nonlinear Dynamics: Integrability, Chaos and Patterns.*(Springer-Verlag, Heidelberg,2005).

[12] H Boris and A Katok, *A First Course in Dynamics: With a Panorama of Recent Developments.* (Cambridge University Press, 2003).

[13] M. Bennett, M.F. Schatz, H. Rockwood and K. Wiesenfeld, Proc. R. Soc. London, A **458**, 563 (2002).

[14] A. Argyris, D. Syvridis, L. Larger, V. Annovazzi-Lodi, P. Colet, I. Fischer, J. Garacia-Ojalvo, C. R. Mirasso, L. Pesquera, and K. A. Shore, Nature **438**, 343 (2005).

[15] P. Mohanty, Nature **437**, 325 (2005).

[16] S. K. Dana, P. K. Roy, and J. Kurths,*Complex Dynamics in Physiological Systems: From Heart to Brain* (Springer, New York, 2009).

[17] H. Fujisaka and T. Yamada, Prog. Theor. Phys. **69**, 32(1983).

[18] T. Yamada and H. Fujisaka, Prog. Theor. Phys. **70**, 1240 (1983).

[19] T. Yamada and H. Fujisaka, Prog. Theor. Phys. **72**, 885 (1984).

[20] H. Fujisaka and T. Yamada, Prog. Theor. Phys. **75**, 1087 (1986).

[21] L.M. Pecora and T.L. Carroll, Phys. Rev. Lett. **64**, 821 (1990).

[22] L.M. Pecora and T.L. Carroll, Phys. Rev. A. **44**, 2374 (1991).

[23] A. Pikovsky, M.Rosenblum and J.Kurths, *Synchronization: A Universal concept in Nonlinear Science* (Cambridge University press, Cambridge, 2001).

[24] S. Boccaletti, J. Kurths, G. Osipov, D.L. Valladares and C.S. Zhou,Phys. Reports **366**, 1 (2002).

[25] K.M. Cuomo and A.V. Oppenheim, Phys. Rev. Lett. 71, 65 (1993).

[26] K.M. Cuomo, A.V. Oppenheim and S.H. Strogatz, IEEE. Trans. Circuit Systems II. 40, 626 (1993).

[27] T. L. Carroll and L. M. Pecora, IEEE Trans. Circuits Syst. **38**, 453 (1991).

[28] H. D. I. Abarbanel, N. F. Rulkov, and M. M. Sushchik, Phys. Rev. E 53,4528 (1996).

[29] N. F. Rulkov, M. M. Sushchik, L. S. Tsimring, and H. D. Abarbanel, Phys.Rev. E 51, 980 (1995).

[30] M. G. Rosenblum, A. S. Pikovsky, and J.Kurths,Phys. Rev. Lett. 76, 1804(1996).

[31] A. A. Koronovskii and A. E. Hramov, Tech. Phys. Lett. 30,587(2004).

[32] V. Belykh, I. Belykh, and M. Hasler, Phys. Rev. E 62, 6332 (2000).

[33] W. Liu, J. Xio, X. Qian, and J. Yang, Phys. Rev. E 73, 057203 (2006).

[34] M. G. Rosenblum, A. S. Pikovsky, and J. Kurths, Phys. Rev. Lett. 78,4193 (1997).

[35] S. Taherion and Y. C. Lai, Phys. Rev. E 59, R6247 (1999).

[36] R. Mainieri and J. Rehacek, Phys. Rev. Lett. 82,3042 (1999).

[37] D. Xu, Phys. Rev. E 63 , 27201(2001).

[38] D. Xu, Z. Li, and S.R. Bishop, Chaos 11, 439 (2001).

[39] D. Xu and C.Y. Chee, Phys. Rev. E 66, 046218 (2002).

[40] Z. Li and D. Xu, Phys. Lett. A 282, 175(2001).

[41] D. Xu, W.L. Ong, and Z. Li, Phys. Lett. A 305,167 (2002).

[42] G. Wen, D. Xu, Chaos Solitons Fractals 26, 71 (2005).

[43] J. Yan, C. Li, Chaos Solitons Fractals 26, 1119 (2005).

[44] G.H. Li, Chaos Solitons Fractals 32 ,1454 (2007).

[45] C.Y. Chee, D. Xu, Chaos Solitons Fractals 23, 1063 (2005).

[46] Z. Li, D. Xu, Chaos Solitons Fractals 22,477 (2004).

[47] M. Hu, Z. Xu, Nonlinear Anal. Real World Appl. 9, 1253 (2008).

[48] A.N. Milioua, I.P. Antoniadesa, S.G. Stavrinides, A.N. Anagnostopoulos, Nonlinear Anal. Real World Appl. 8,1003 (2007).

[49] G.H. Li, Chaos Solitons Fractals 32,1454 (2007).

[50] G.H. Li, Chaos Solitons Fractals 32,1786 (2007).

[51] M. Hu, Z. Xu, R. Zhang, and A. Hu, Phys. Lett. A 361, 231 (2007).

[52] J. H. Park, Chaos Solitons Fractals 34,1154(2007).

[53] J. H. Park, J Comput Appl Math 213,288 (2008).

[54] A. E. Hramov and A. A. Koronovskii, Chaos 14, 603 (2004).

[55] A. E. Hramov, A. A. Koronovskii, P. V. Popov, and I. S. Rempen, Chaos 15, 013705 (2005).

[56] A. E. Hramov, A. A. Koronovskii, M. K. Kurovskaya, and O. I. Moskalenko, Phys. Rev. E 71, 056204 (2005).

[57] A. E. Hramov and A. A. Koronovskii, Physica D 206, 252 (2005).

[58] A. E. Hramov, A. A. Koronovskii, and Y. I. Levin, JETP 100, 784 (2005).

[59] R-h Li, Appl. Math. Comput. 200, 321 (2008)

[60] H. Du, Q. Zeng, C. Wong, Phys. Lett. A 372, 5402 (2008).

[61] L. Runzi, Phys. Lett. A 372, 3667(2008).

[62] H. Du, Q. Zeng, C. Wong, Chaos Solitons Fractals 42,2399 (2009) .

[63] E. Ott, C. Grebogi, and J. A. Yorke, Phys. Rev. Lett.**64**,1196(1990).

[64] Y. Lai and C. Grebogi, Phys. Rev. E 47, 2357(1993).

[65] J. H. Peng, E. J. Ding,M. Ding, and W. Yang, Phys. Rev. Lett. **76**, 904 (1996).

[66] S. H. Chen and D. X. Wang, Chaos **14**, 539(2004)

[67] J. F. Heagy, T. L. Caroll, and L. M. Recora, Phys. Rev. E **50**, 1874(1994)

[68] J. F. Heagy, T. L. Caroll, and L. M. Recora, Phys.Rev. Lett. **73**,3528 (1994).

[69] J. Q. Fang, Y. Hong,G. Chen, Phs. Rev. E 59, R2523 (1999).

[70] X. Yu, G. Chen, Y. Xia, Y. X. Song, and Z. W. Cao, IEEE Trans. Circuits Syst., I: Fundam. Theory Appl. 48, 930(2001).

[71] K. Tanaka and H.O. Wang, IEEE World Congress on Fuzzy Systems Proceedings, 1,434(1998).

[72] K. Y. Lian, T. S. Chiang, C. S. Chiu, and P. Liu, IEEE Trans. Syst. Man Cybern. B 31, 66 (2001).

[73] T. Yang and L. O. Chua, IEEE Trans. Circuits Syst., I: Fundam. Theory Appl. 44, 976 (1997).

[74] T. Yang, L. B. Yang, and C. M. Yang, Physica D 110, 18 (1997).

[75] E. W. Bai and K. E. Lonngren, Chaos, Solitons Fractals 8, 51 (1997).

[76] E. W. Bai and K. E. Lonngren, Chaos, Solitons Fractals 11, 1041 (2000).

[77] H. N. Agiza and M. T. Yassen, Phys. Lett. A 278, 191 (2001).

[78] E.W. Bai, K.E. Lonngren and J.C. Sprott, Chaos, Solitons Fractals 13,1515 (2002).

[79] H.K. Chen, Chaos, Solitons Fractals 25,1049 (2005).

[80] U.E. Vincent, Phys. Lett. A 343,133 (2005).

[81] A. Ucar, E.W. Bai and K.E. Lonngren, Phys. Lett. A 314,96 (2003).

[82] A. Ucar, K.E. Lonngren and E.W. Bai, Chaos Solitons Fractals 31,105(2007).

[83] U. E. Vincent and J. A. Laoye, Physica A 384,230(2007).

[84] U. E. Vincent and J. A. Laoye, Phys. Lett. A 363,91(2007).

[85] A. N. Njah and U. E. Vincent, Journal of sound and vibration 319, 41(2009).

[86] T. Kapitaniak, Chaos Solitons Fractals 6,237(1995).

[87] M. D. Bernardo, Int. J. of Bifurcation and Chaos Appl. Sci. Eng.6, 557(1996).

[88] C. W. Wu, T. Yang, L. O. Chua, Int. J. of Bifurcation and Chaos Appl. Sci. Eng.6, 455(1996).

[89] T.L. Liao and S.-H. Lin, J. Frankli Inst. 336, 925(1999).

[90] M.T. Yassen, Appl. Math. Comput. 135, 113 (2001).

[91] A. S. Hegazi, H. N. Agiza, and M. El-Dessoky, Int. J. Bifurcation Chaos Appl. Sci. Eng. 12, 1579 (2002).

[92] Z. Li, C. Han and S. Shi, Phys. Lett. A 301, 224(2002).

[93] Y. Wang, Z.H. Guan and H. O. Wang, Phys. Lett. A 312,34(2003).

[94] S. H. Chen, J.Hu, C. P.Wang, and J. H. L, Phys. Lett. A 321, 50 (2004).

[95] D. B. Huang and R. W. Guo,Chaos 14, 152 (2004).

[96] D. B. Huang,Phys.Rev. E 71, 037203 (2005).

[97] M.T. Yassen, Phys. Lett A 337, 335(2005).

[98] H. Zhang, W. Huang, Z. wang and T.Chai, Phys. Lett. A 350, 363(2006).

[99] S. Li, W. Xu, and R. Li, Phys. Lett A 361, 98(2007).

[100] X. Chen and J. Lu, Phys. Lett. A 364, 123(2007).

[101] J. Lasalle and S. Lefschtg, Stability by Lyapunovs Direct Method with Application (Academic, New York, 1961).

[102] J. D. Cao, H. X. Li, and D. W. C. Ho, Chaos, Solitons Fractals 23, 1285 (2005).

[103] J. H. Park and O. M. Kwon, Chaos, Solitons Fractals 23, 445 (2005).

[104] E. A. Jackson ,I. Grosu, Physica D 85,1(1995).

[105] I. Grosu , Phys. Rev. E 56, 3709(1997).

[106] G. Chen, X.Dong, *From Chaos to Order - Perspectives, Methodologies, Applications* (World Scientific,Singapore, 1998)

[107] L. Q. Chen ,Y. Z. Liu , Int. J. Bifurcation Chaos Appl. Sci. Eng 12(5),1219 (2002).

[108] A. I. Lerescu, N. Constandache, S. Oancea, I. Grosu, Chaos, Solitons Fractals 22(3), 599 (2004).

[109] I. Grosu,Int. J. Bifurcation Chaos Appl. Sci. Eng. 17, 3519(2007).

[110] C. Li, W. Sun, and J. Kurths, Phys. Rev. E 76, 046204(2007).

[111] I. Grosu, E. Padmanaban, P. K. Roy, and S. K. Dana, Phys. Rev. Lett.100, 234102 (2008).

[112] I. Grosu, R. Banerjee, P. K. Roy, and S. K. Dana, Phys. Rev. E 80,016242 (2009).

[113] J.H.Mathews, *Numerical Methods for Mathematics, Science and Engineering* (Prentice-Hall of India, New Delhi, 1998).

[114] F. Luigi, P. Domenico, Int. J. Bifur. Chaos 14 (3), 1085(2004).

[115] Z. Ge, C. Yang, Phys. Lett. A 373, 349 (2009)

[116] O. E. Rössler, Phys. Lett. A 57, 397 (1976).

[117] J. Lü, G. Chen, Int. J. Bifurcat. Chaos 12, 659(2002).

[118] J. Lü, G. Chen, S. Zhang, Int. J. Bifurcat. Chaos 12, 1001(2002).

[119] A. Chen, J. Lu, J. Lu, S. Yu, Physica A 364, 103(2006).

[120] T. Gao, G. Chen, Z. Chen, S. Cang, Phys. Lett. A 361,78 (2007) .

[121] Z. Yan, Appl. Math. Comput. 168, 1239(2005).

[122] O. E. Rössler, Phys. Lett. A 7, 155(1979) .